Joint European Summer School for
Fuel Cell and Hydrogen Technology
Heraklion, Crete
21st September 2012

JÜLICH
FORSCHUNGSZENTRUM

Characterization Methods

In-situ Methods

Robert Mücke

Forschungszentrum Jülich GmbH, Institute of Energy and Climate Research
(IEK-1: Materials Synthesis and Processing)

Why *in situ* Methods?

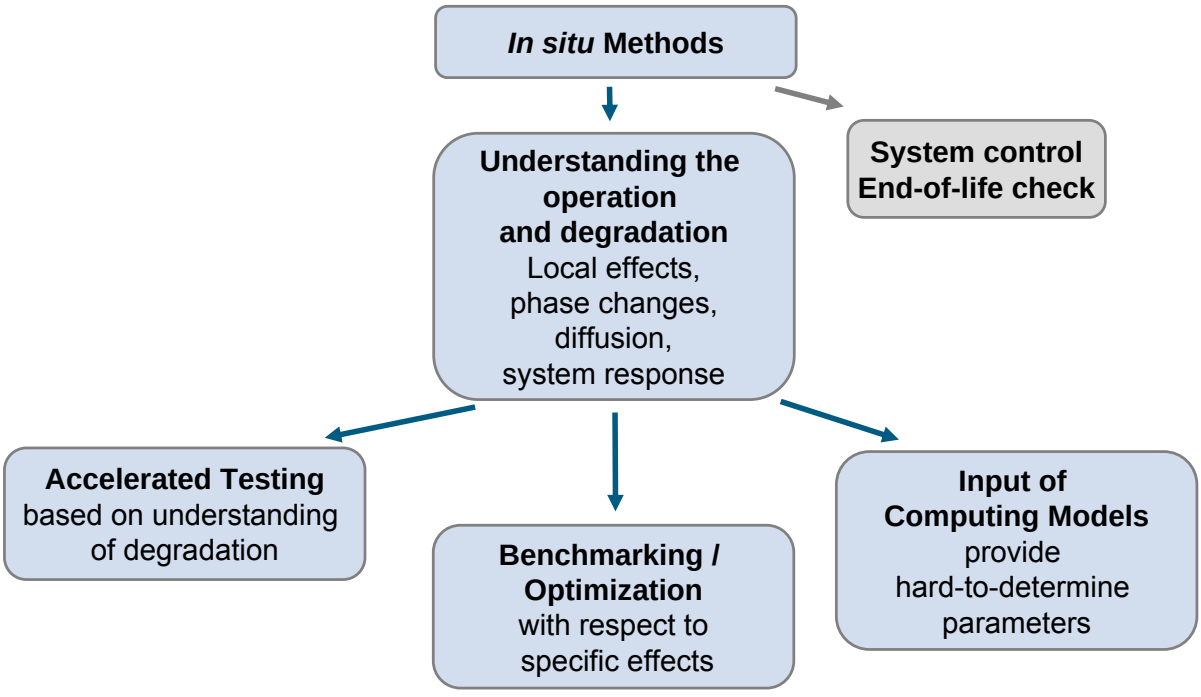

Overview

Technique	Observable(s)	Pro	Cons
Electrochemical voltammetry	Current and power density	Ultimate performance metric	Often chemically ambiguous and model specific
Impedance spectroscopy	Cell and electrolyte resistance	Activation barriers and ohmic losses	Often chemically ambiguous and model specific
Products			
Mass spectroscopy Gas chromatography	Gas products and fuel utilization	Monitors efficiency	Indirect, vulnerable to interferences
XRD	Phase structure, stresses	Chemically specific	Only for crystalline
XPS	Material compos. and structure	Material specific	Challenging in situ, elemental rather than molecular information
EXAFS, XANES	Composition and adsorbates, oxidation states	Chemically specific	Challenging for experiments and interpretation

extended, after Pomfret et al, Annu. Rev. Anal. Chem. 2010. 3:151–74

Overview

Technique	Observable(s)	Pro	Cons
Optical			
Raman spectroscopy	Composition, structure, temperature, stresses of mater. and adsorbates	Molecular and material specific, kinetics, real time	Used for a single position at a time
Infrared spectroscopy	Surface species	Adsorbate structure specific, broad spatial coverage, real time	Experimentally challenging
Imaging (vis+IR)	Emission, temperature	Spatially resolved, real time	Lacks molecular specificity
Radiography / Tomography		penetrating bulk	element spec. only
X-Ray CT/synchrotron	Contrast by atomic number (e shell)	high resolution (0.5-2 µm)	weak contrast for adjacent elements
Thermal neutrons	Contrast by nucleus interaction	often contrasts adjacent elements	low resolut. (>30µm) more expensive
NMR	Magnetic spin of nucleus	high resolut. (1-3µm) smaller devices	no ferror-magnetic materials, small scale

Treated Methods in More Detail

1. Temperature & Optical Access
2. Electrochemical Impedance Spectroscopy
3. Local Measurements
   (Current Distribution, Voltammetry, Gas Analysis)
4. Radiography & Tomographic Imaging
   - Computed Tomography / X-Ray Imaging
   - Synchrotron Tomography
   - Neutron Imaging
   - Nuclear Magnetic Resonance Imaging (NMR)
5. X-Ray Diffraction and Spectroscopy (XRD, XAS, XPS)
6. Raman Spectroscopy
7. Scanning Probe Microscopes

1. Temperature and Optical Access

The Easiest in situ Measurement Temperature (SOFC)

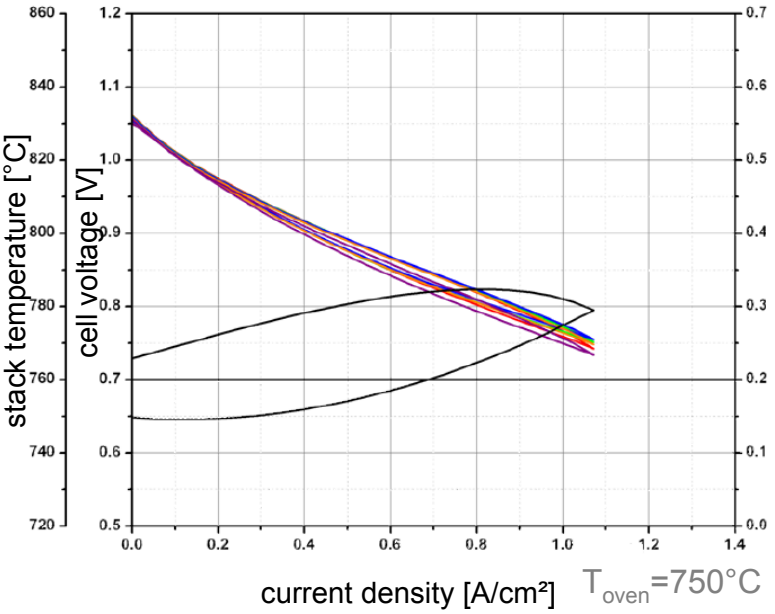

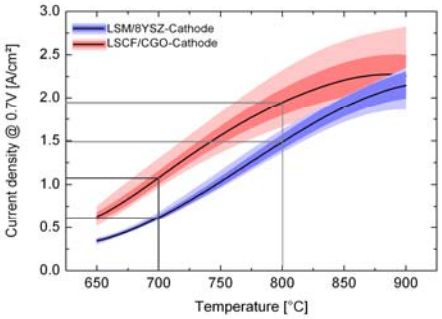

temperature influences conductivity and electro-chemistry
=> *T* should be monitored for *i-V* curves

SOFC Stack Temperature In Plane Distribution

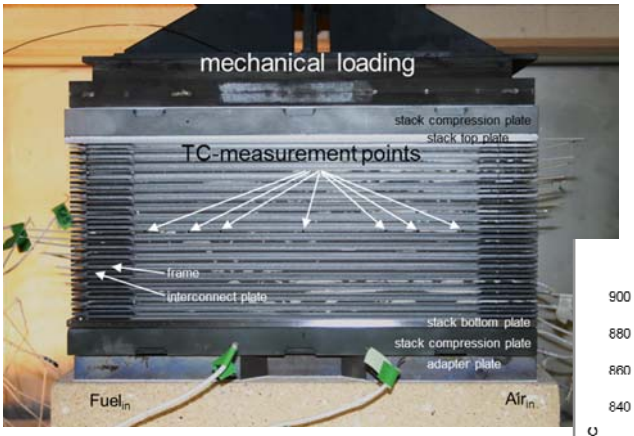

endothermic reactions when reforming CH_4

$\Rightarrow$ larger ΔT

depends on u_F
(less fuel, less reforming)

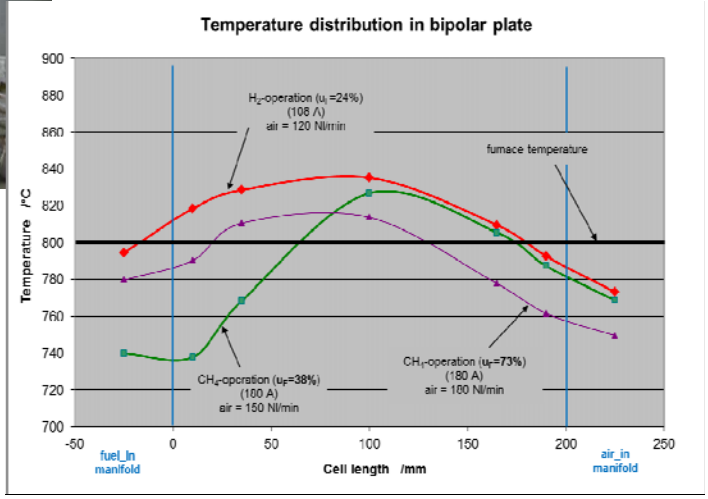

ΔT upto 100K can occur

$\Rightarrow$ critical for mechanical integrity esp. glass sealings

special interconnects required

L. Blum et al., 10th European SOFC Forum Lucerne 2012, A0405

SOFC Stack Temperature Height Distribution

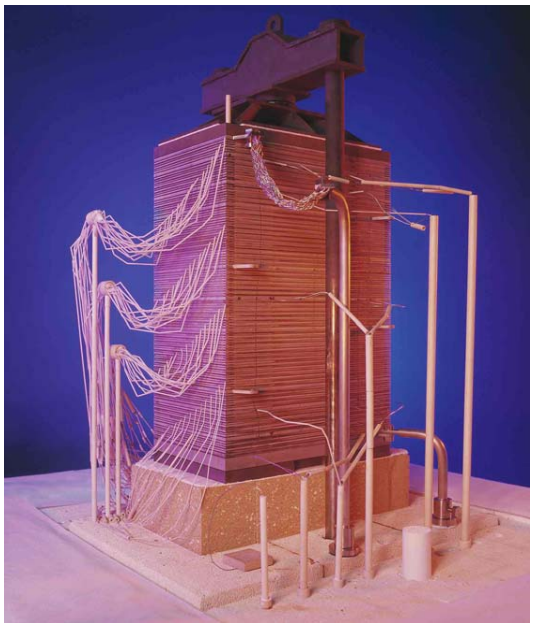

60 cell stack

Optical Access In Plane

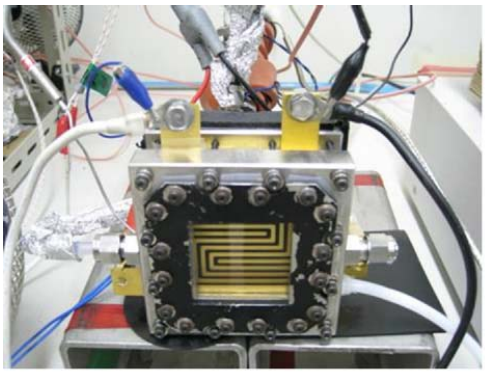

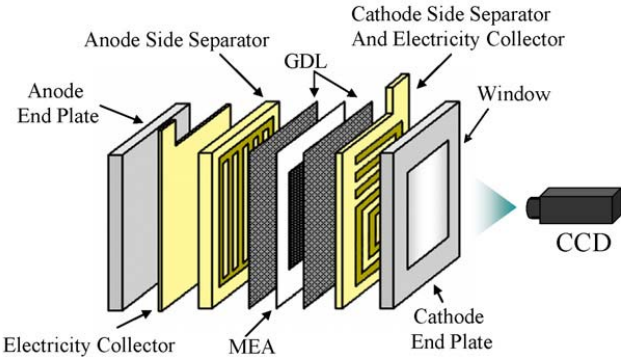

special transparant window required

only specific layers accessible (GDL)

K.S.S. Naing et al. / Journal of Power Sources 196 (2011) 2584–2594
cf. Bazylak, Int. J. Hydr. Energy 34 (2009), 3845-3857 (review)
Rosli et al., J. Fuel Cell Sci. Technol. 7 (2010), 061015-1

Optical Access In Plane

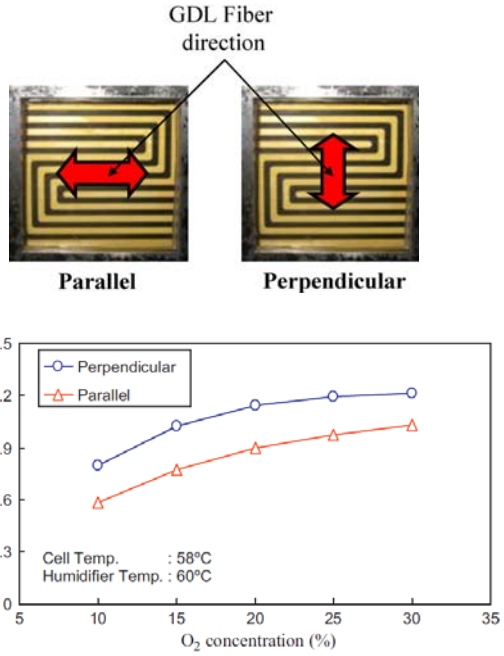

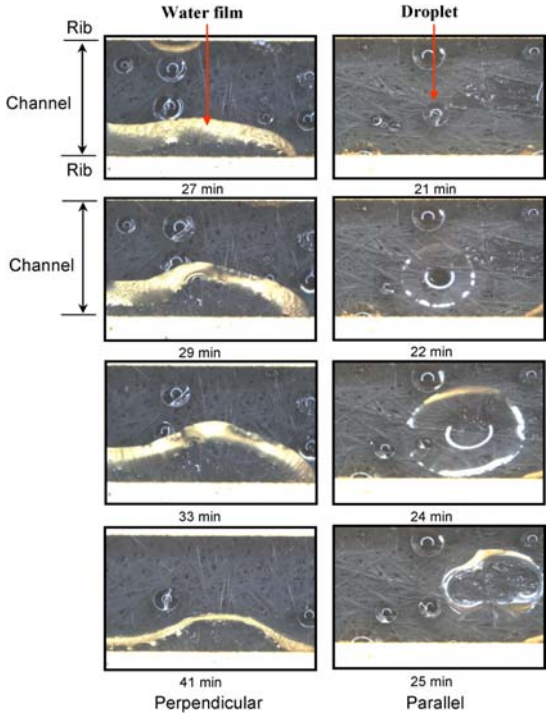

K.S.S. Naing et al. / Journal of Power Sources 196 (2011) 2584–2594

Optical Access Through Plane

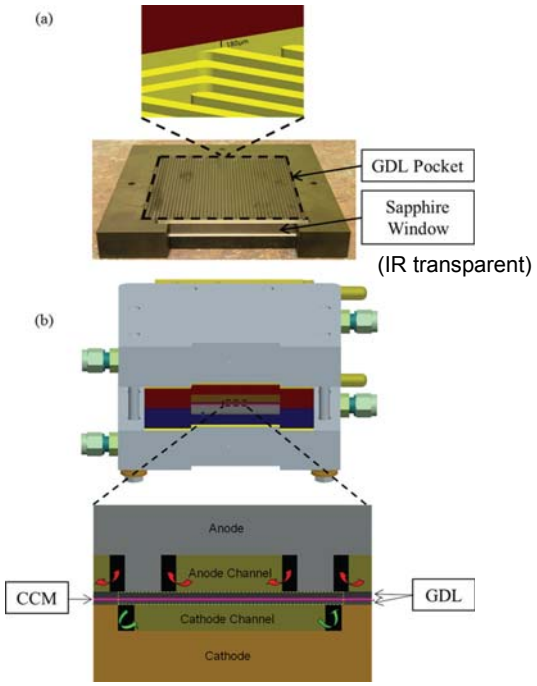

water in cathode GDL

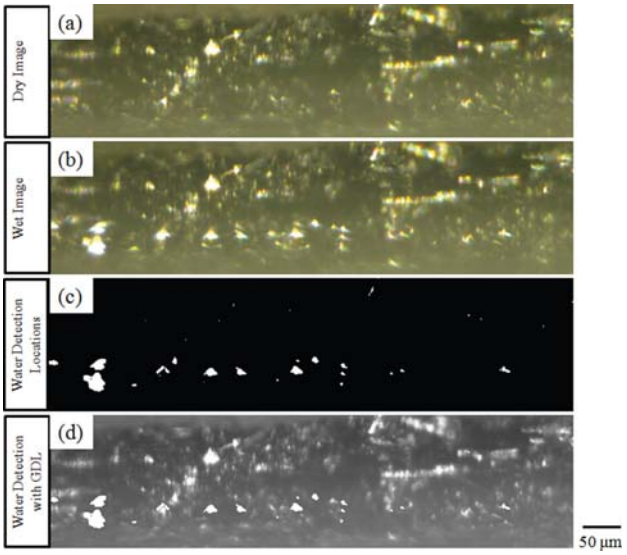

differential imaging
(subtracting before and after)

Daino et al., Electrochemical and Solid-State Letters, 14 (6) B51-B54 (2011)

Optical Access
Through Plane (Cross Section)

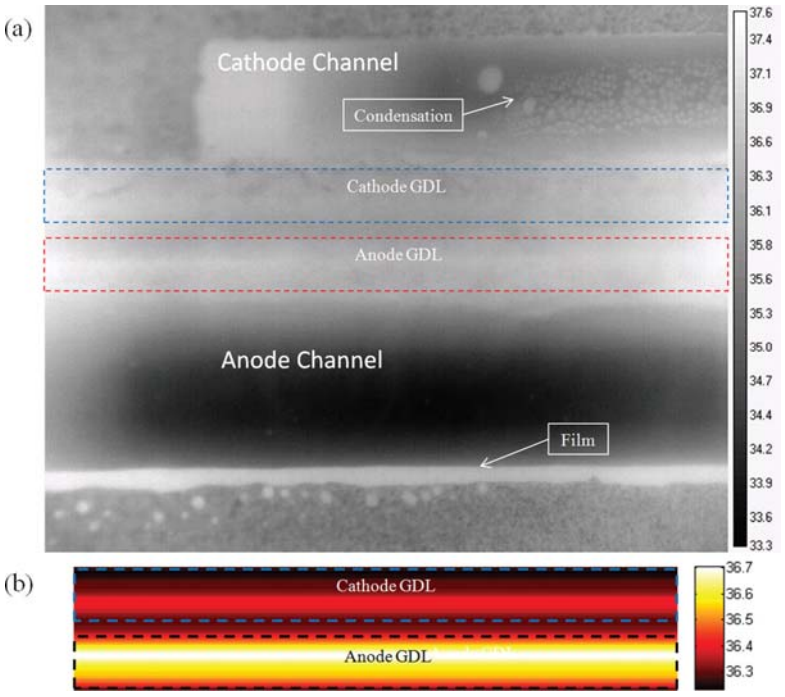

thermal imaging:

0.1K resolution possible
critical point:
unknown emissivities

Daino et al., Electrochemical and Solid-State Letters, 14 (6) B51-B54 (2011)

2. Electrochemical Impedance Spectroscopy

"Insights" without direct access

Extended Model for Reformate Fuels

All Reasonable EIS characterization Require a Model!

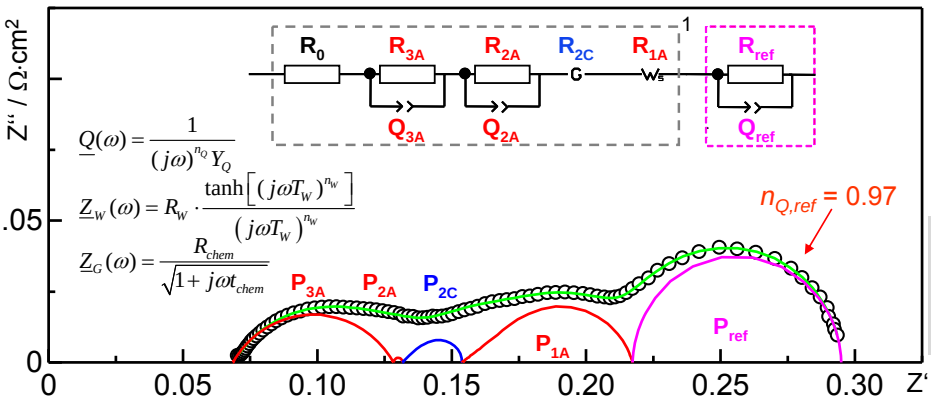

$$\underline{Q}(\omega) = \frac{1}{(j\omega)^{n_Q} Y_Q}$$

$$\underline{Z}_W(\omega) = R_W \cdot \frac{\tanh\left[(j\omega T_W)^{n_W}\right]}{(j\omega T_W)^{n_W}}$$

$$\underline{Z}_G(\omega) = \frac{R_{chem}}{\sqrt{1 + j\omega t_{chem}}}$$

cell type: FZJ-ASC
el. area: 1 cm²
fuel: 15% H_2, 5% H_2O, 15% CO, 5% CO_2, 60% N_2, 250 sccm
oxidant: air, 250 sccm
T = 800 °C
OCV

measured spectrum
CNLS-Fit
anode process
cathode process

Process	Dependence	Physical Origin	Equivalent Circuit Element
P_{2C}	$pO_{2.cat}$, T	oxygen surface exchange kinetics and bulk diffusion of O^{2-}	Gerischer-Element
P_{ref}	$pH_{2.an}$, pH_2O_{an}, T (low)	coupling of CO-shift & CO/CO_2 diffusion	**RQ-Element**
P_{1A}	$pH_{2.an}$, pH_2O_{an}, T (low)	gas diffusion (anode substrate)	GFLW-Element
P_{2A}	$pH_{2.an}$, pH_2O_{an}, T	gas diffusion coupled with charge transfer reaction and ionic transport	serial connection of RQ_{2A} & RQ_{3A}
P_{3A}	$pH_{2.an}$, pH_2O_{an}, T		

A. Kromp, A. Leonide, A. Weber, E. Ivers-Tiffée, J. Electrochem. Soc., 158 (8), B980-B986, (2011).
A. Kromp, A. Leonide, H. Timmermann, A. Weber and E. Ivers-Tiffée, ECS Trans., 28, 205 (2010).

Reformate Gas Impedance

Subtracted Impedance Spectra

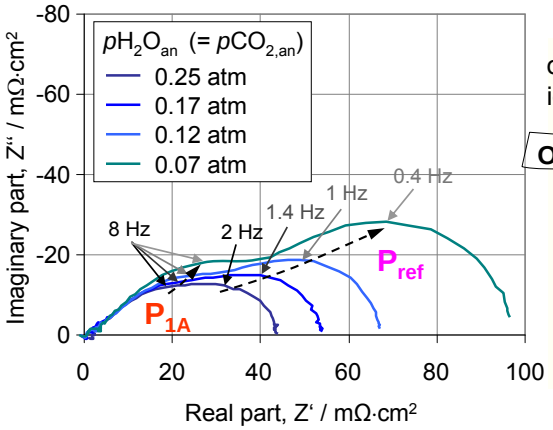

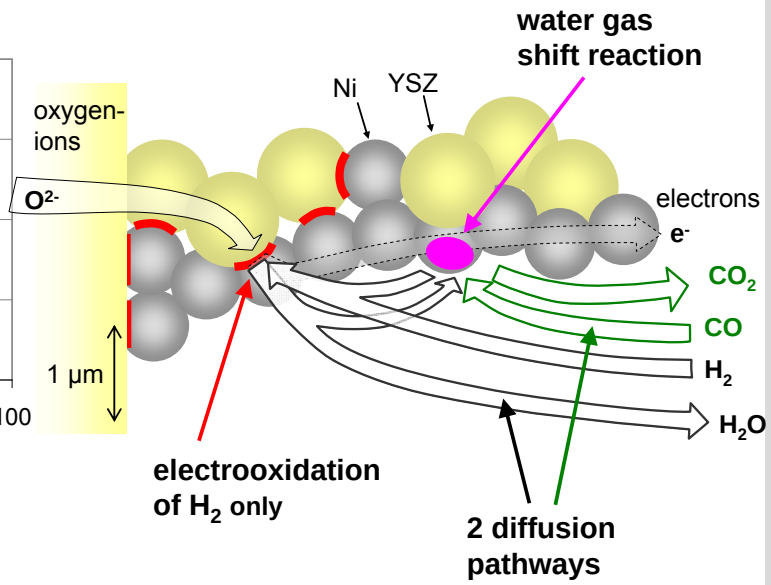

2 Polarization Processes

- H_2/H_2O diffusion P_{1A} clearly visible
- f(P_{ref}) = 0.4 .. 2 Hz → CO/CO_2 diffusion[1]
- reforming reactions

→ P_{ref}: Coupling of shift-reaction & CO/CO_2 diffusion

Stability in Reformate

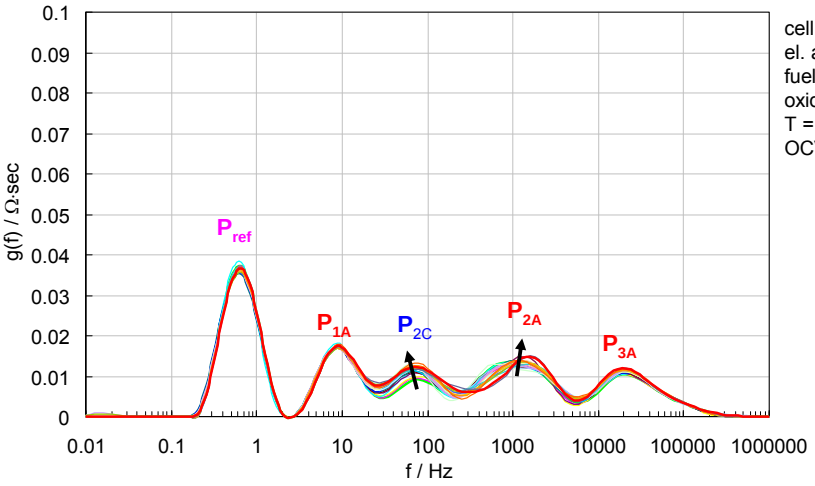

cell type: FZJ-ASC
el. area: 1 cm²
fuel: reformate, 250 sccm
oxidant: air, 250 sccm
T = 800 °C
OCV

- degradation of the cathode as usual
- no severe degradation of the anode

Stability in Reformate with 0.5 ppm H_2S

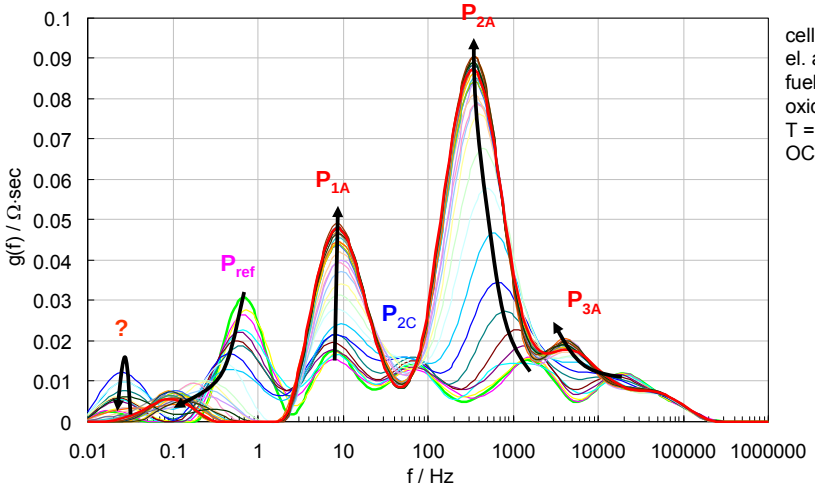

cell type: FZJ-ASC
el. area: 1 cm²
fuel: reformate + 0.5 ppm H_2S, 250 sccm
oxidant: air, 250 sccm
T = 800 °C
OCV

could be verified by mass spectroscopy/ gas chromatography (general problem H_2O condensation)

- severe degradation of P_{2A} (H_2 electrooxidation)
- increase of P_{1A} (H_2/H_2O gas diffusion in anode substrate)
- decrease of P_{ref} (no CO-shift → no CO/CO_2 gas diffusion → similar to inert gas)

3. Local Electrochemical and Products Measurements

Local Current Measurement (PEMFC)

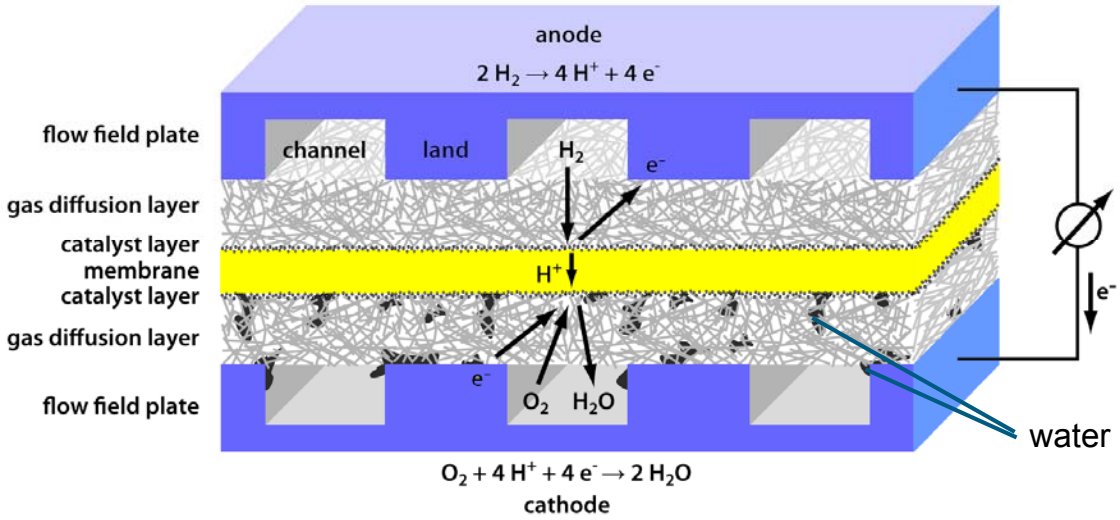

goals: check flow field, local fuel utilization / fuel supply
local channel/land effects

Local Current Measurement Parallel to Flow Channels

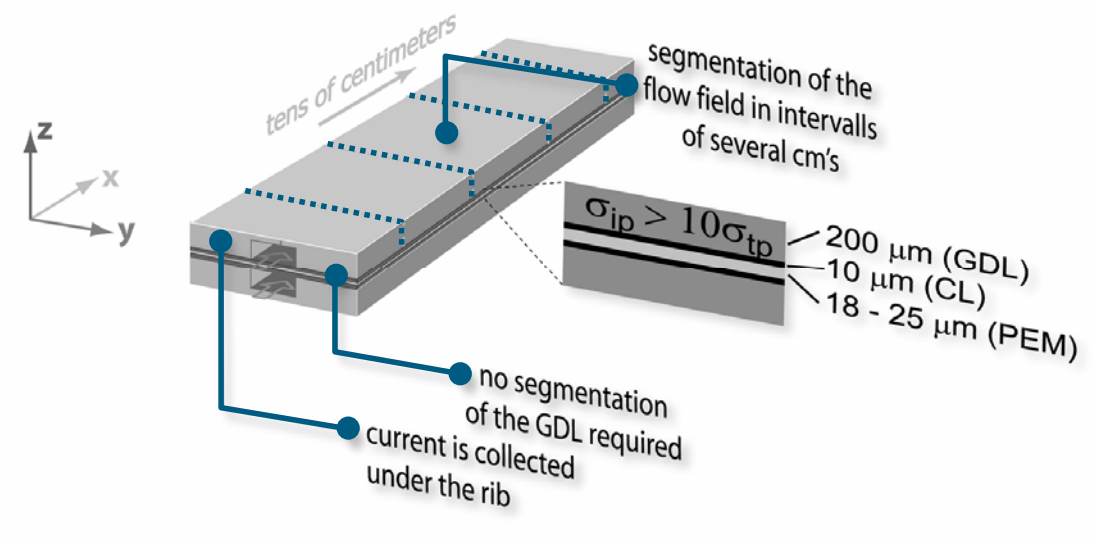

Segmentation in range of several cm >100x GDL thickness
→ only small compensating currents → no GDL segmentation required

S. von Dahlen, PhD thesis, ETH Zürich, 2012

Local Current Measurement Large Segments

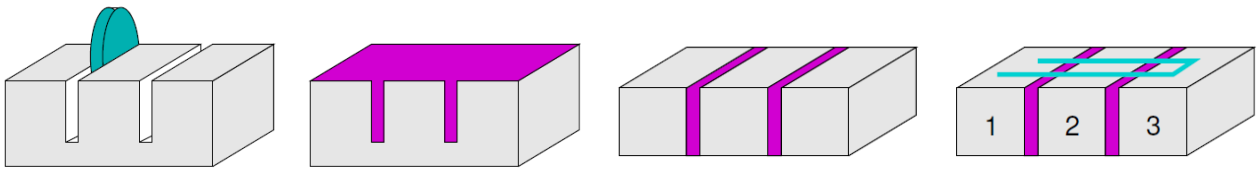

mill channel | fill with adhesive | mill both sides | mill flow field

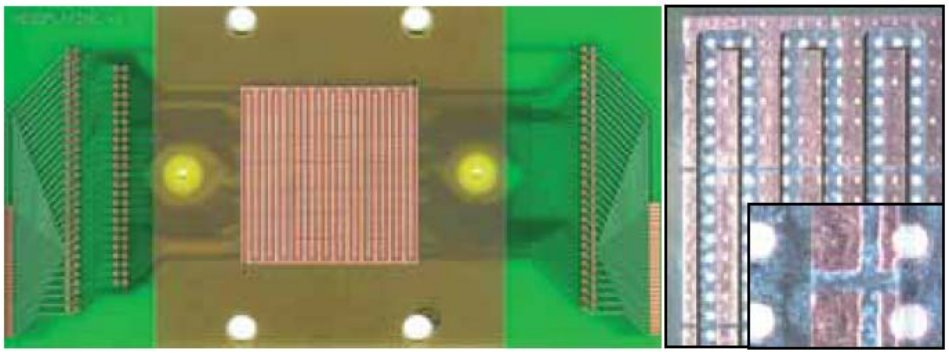

milled, etched, integrated T sensors

comprehensive 7x7 segmented flow field plate

H. Kuhn, PhD thesis, ETH Zürich, 2006
Schönbauer, PhD thesis, Univ. Stuttgart, 2009
cf. I.A. Schneider et al., J. Electrochem. Soc. 154 (8) B770-B782 (2007)

Local Current Measurement Large Segments

7x7 segmented flow field plate

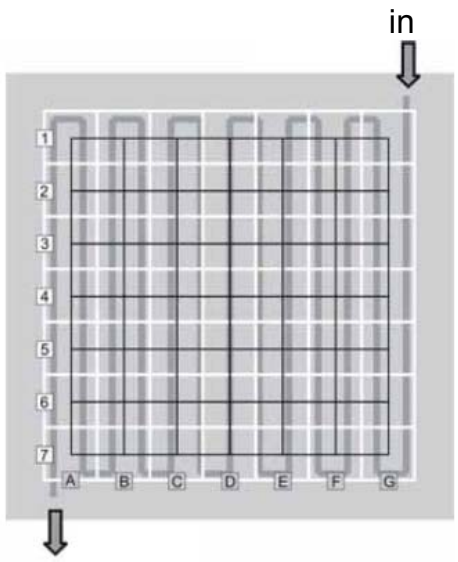

influence of air excess (λ factor)

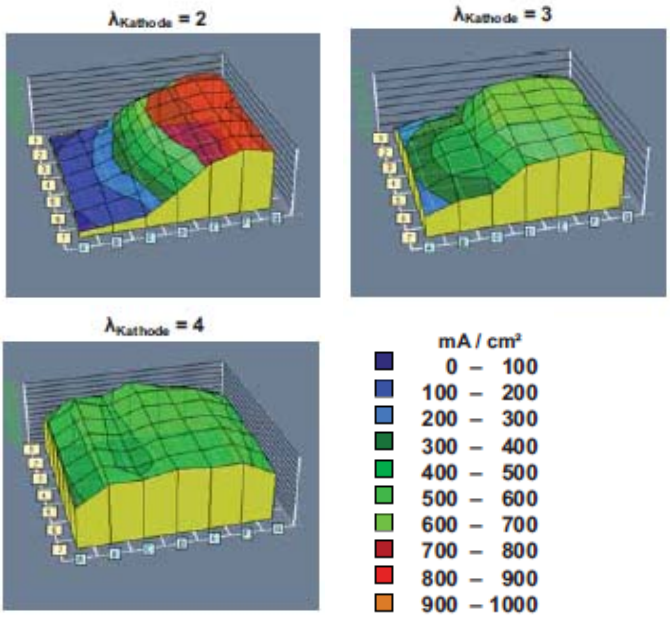

Schönbauer, PhD thesis, Univ. Stuttgart, 2009

Local Current Measurement (SOFC) Large Segments

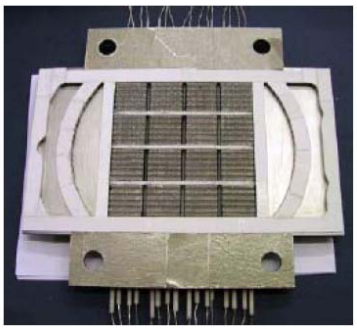

4x4 segmented interconnect

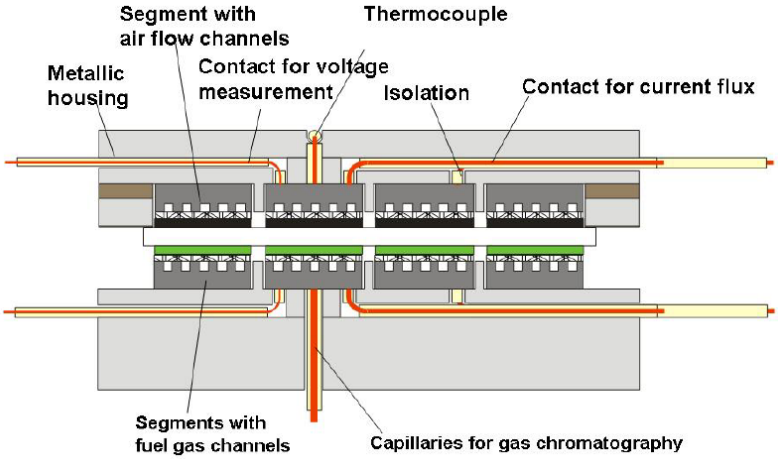

ASC: segmented cathode

ESC: segmented anode/cathode

G. Schiller, DLR Stuttgart, EFCF Lucerne 2010

Local Current Measurement (SOFC)
Large Segments

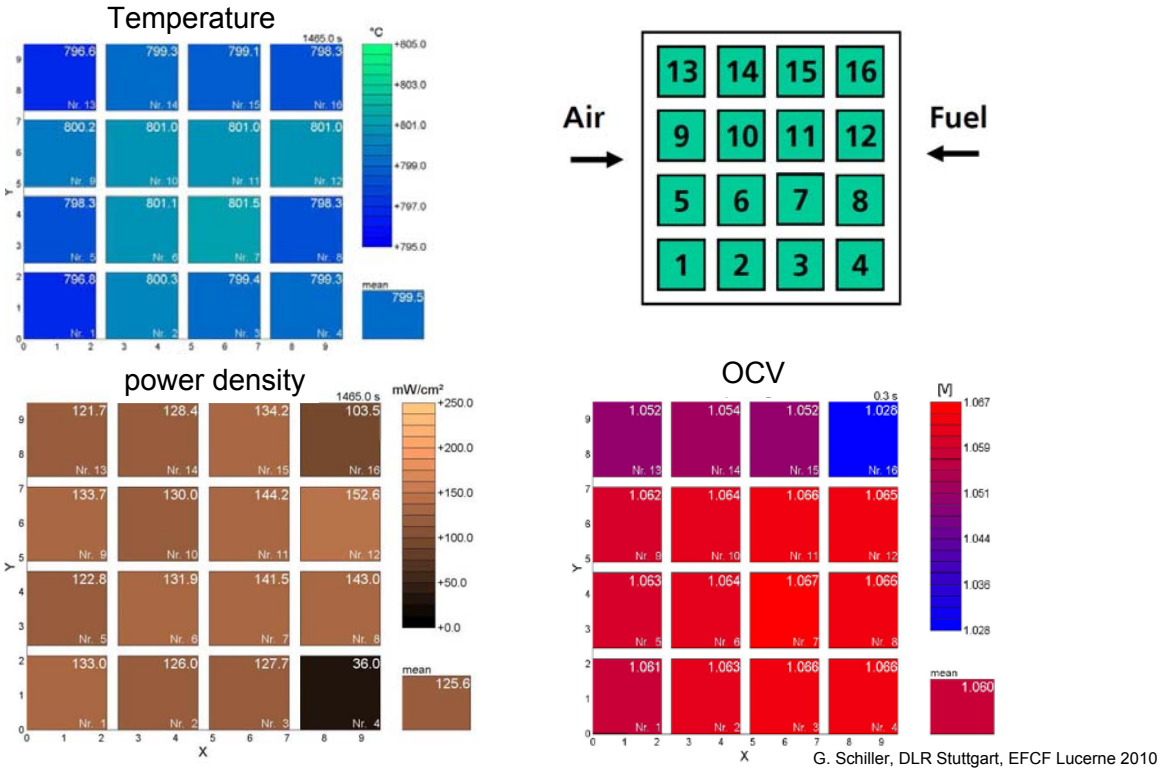

G. Schiller, DLR Stuttgart, EFCF Lucerne 2010

Local Current Measurement
Perpendicular to Flow Channels

Segmentation << 1 mm required

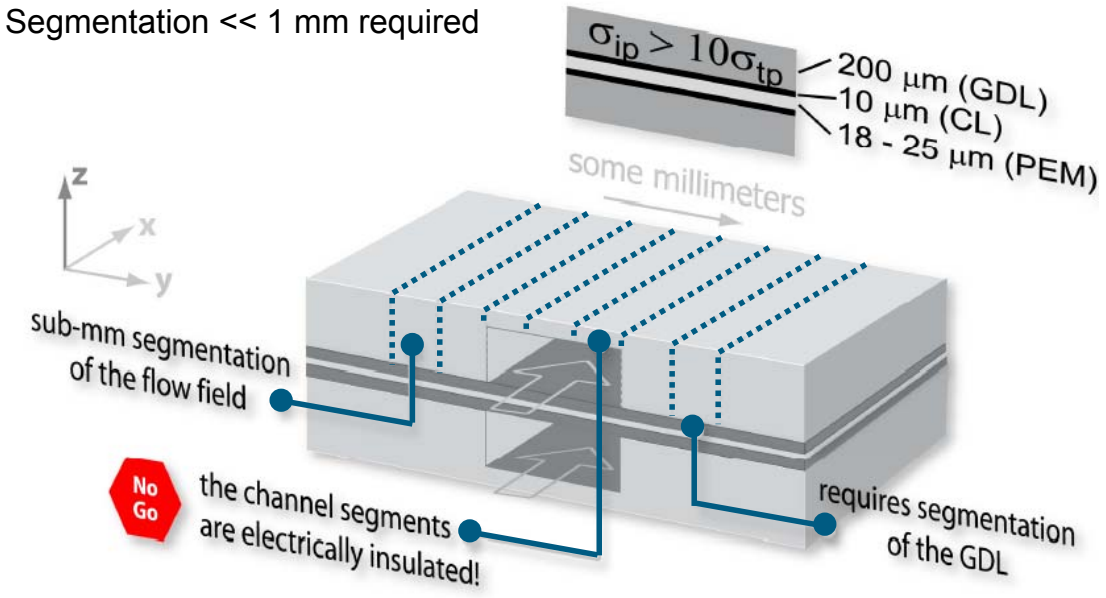

S. von Dahlen, PhD thesis, ETH Zürich, 2012

Local Current Measurement Perpendicular to Flow Channels

Gold wires (25µm) between GDL and catalyst coated membrane

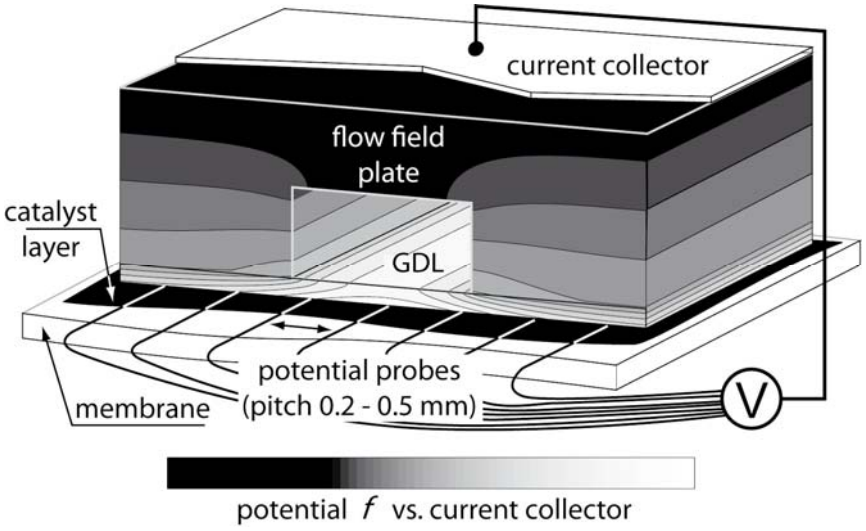

- current calc. from V
- requires modeling of 2D resistance (strongly depends on humidity, mech. load, contact resist.)
- bad s/n ratio
- showed mass transport limitation in land region for humidified gases
- channel regions affected by dry gases
- optimization of flow field geometry

Freunberer et al., J. Electrochem. Soc. 153 (2006), A2158

Local Current Measurement Perpendicular to Flow Channels

micro flow field plate on anode side

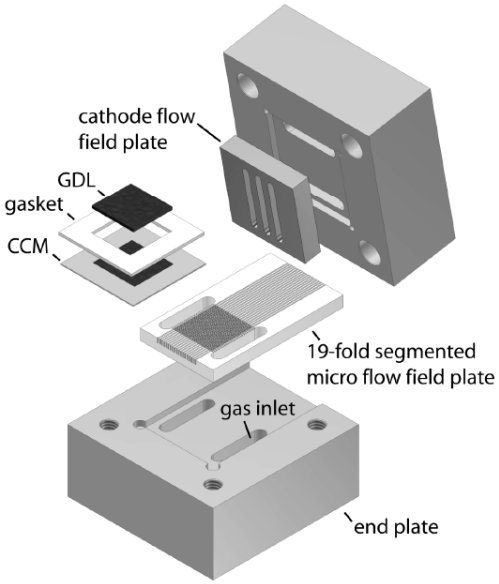

CCM: catalyst coated membrane

most losses on cathode side

quasi homogeneous anode (much thinner channels)

H2 diffuses into Au pinned structure

fully humidified H2 => no GDL on anode side requ. (cross currents of catalyst layer can be neglected)

S. von Dahlen, PhD thesis, ETH Zürich, 2012

Local Current Measurement Perpendicular to Flow Channels

glass ceramic
milling channels (200µmx800µm distance 200µm)
fill with Au, polish
mill 150µm x150µm between Au parallel + perpendicular

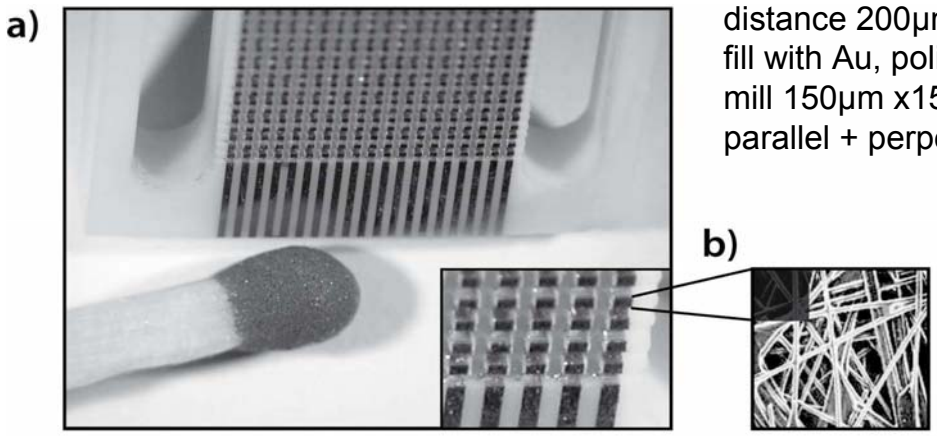

microstructure anodic flow field plate

pin size compared to GDL fibers

current measurement:
high precision shunt resistors (20 mΩ)

S. von Dahlen, PhD thesis, ETH Zürich, 2012

Local Current Measurement Gas and Channel Width Variation

channel width 2 mm

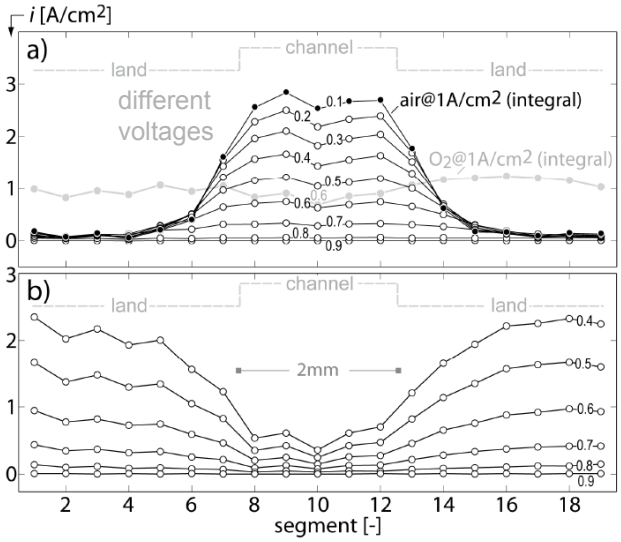

channel width 1.2 mm

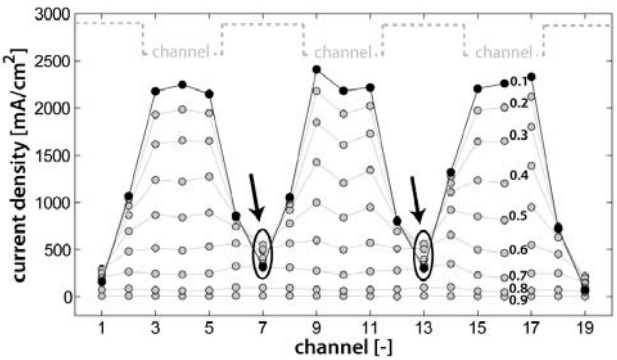

humidified gases air/H_2

a) humidified gases (gray: O_2/H_2, black: air/H_2)
b) dry O_2, 50% H_2O/H_2

further investigations made with local EIS

several flow field geometries tested (parallel, serpentine, interdigitated)

S. von Dahlen, PhD thesis, ETH Zürich, 2012

Local Current Measurement
Transient Start/Stop Behavior

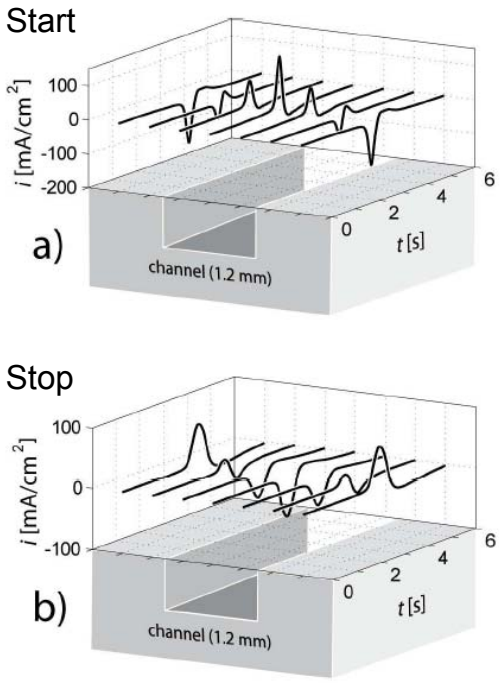

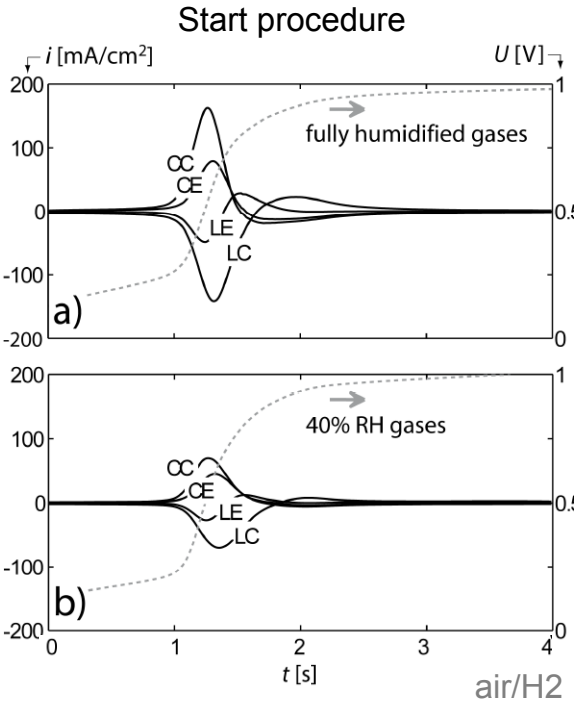

H_2 regions cause neg. current in H_2 poor regions

Cyclic Voltammetry

primarily used to get electrochemical available surface area (ECSA)
start/stop cycles → carbon corrosion → loss of Pt particles → decrease of ECSA
can be extended to local distribution

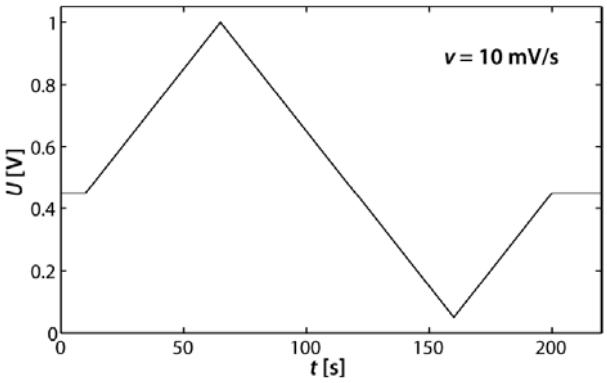

linear sweep waveform

anode (CE): H_2 (fully humidified)
cathode (WE): N_2 (fully humidified)
no O_2 to avoid superposition with O_2 reduction reaction

S. von Dahlen, PhD thesis, ETH Zürich, 2012

Cyclic Voltammetry

measure the chemsorption of H_2 on Pt surface

cyclic voltammogram

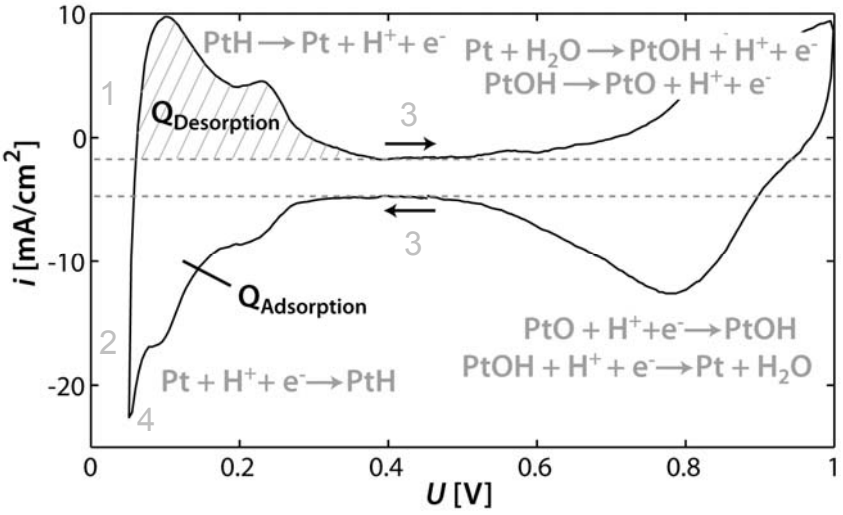

$$Q_{\text{Desorption}} = \frac{1}{v}\int_{\text{upd}} (j - j_{\text{dl}})\,\mathrm{d}V$$

$$ECSA = \frac{Q_{\text{Desorption}}}{e \cdot N_{\text{Pt}}} \quad [\text{cm}^2]$$

Atoms Pt per cm² (poly crystalline):

$$N_{\text{Pt}} = 1.3 \cdot 10^{15}\,\text{cm}^{-2}$$

1: anodic current
2: cathodic current
3: polarization of double layer (no chem. reaction)
4: V < RHE => H_2 formation on WE

upd: underpotentially deposited (=mono layer, lower potential than for next layer)

S. von Dahlen, PhD thesis, ETH Zürich, 2012

Cyclic Voltammetry
H_2 Reduction Currents

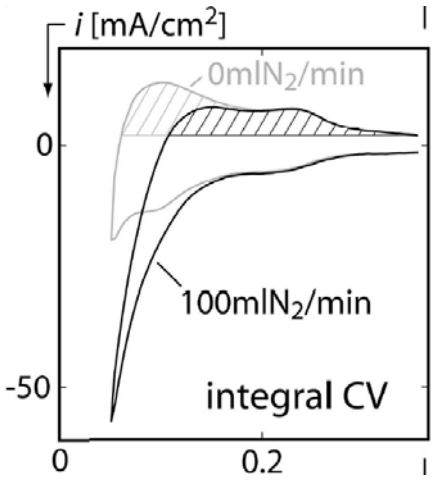

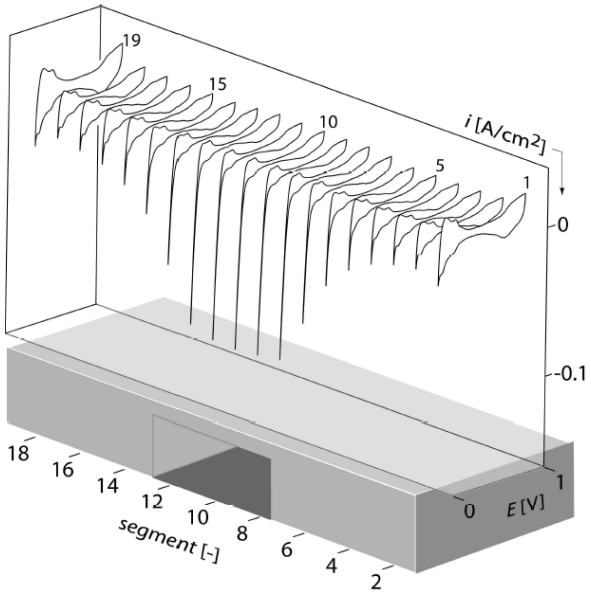

N_2 transports H_2 away
⇒ drastic change of upd area
⇒ underestimating ECSA
⇒ method only accurate for resting atmospheres (impossible in stack)

large cathodic current variation due to N_2 flux

S. von Dahlen, PhD thesis, ETH Zürich, 2012

Electrochemical Available Surface Area via CO stripping

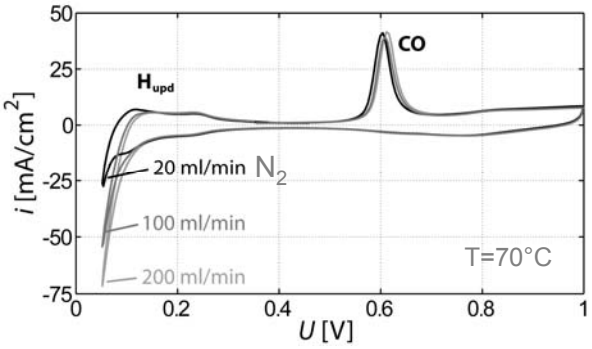

relative *ECSA*

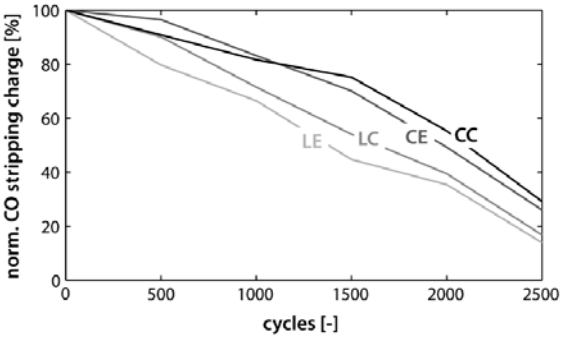

purging: 5 min N_2,
5 min 1% CO => CO mono layer on Pt,
5 min N_2 (CO removal in GDL)

CO desorps at ~0.6 V

CO peak independent of N_2
(H_{upd} not)

CC: channel center
CE: channel edge
LE: land edge
LC: land center

higher degradation at land region
negative current in lands during start higher than negative currents in channels during stop

S. von Dahlen, PhD thesis, ETH Zürich, 2012

Local Gas Phase Measurements

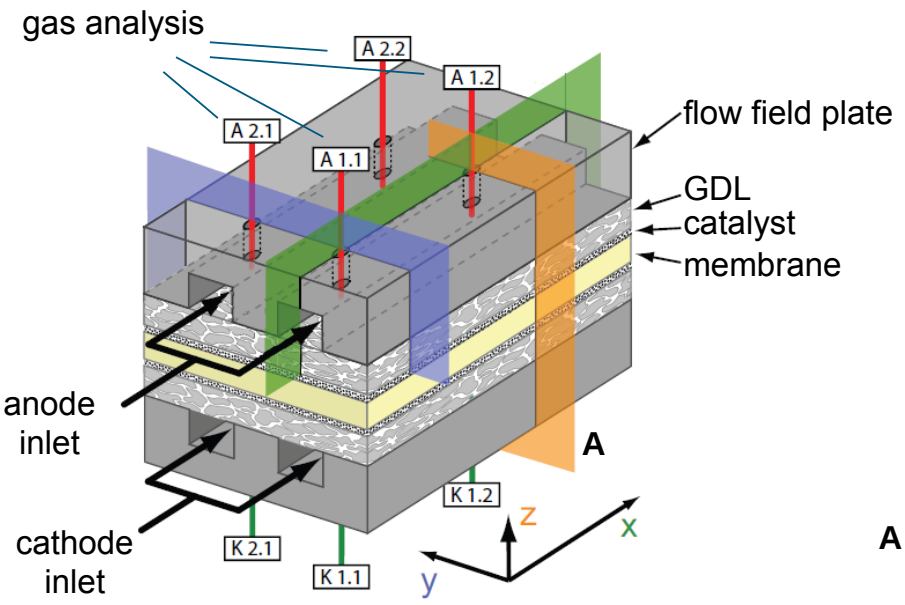

measure gas species along channel

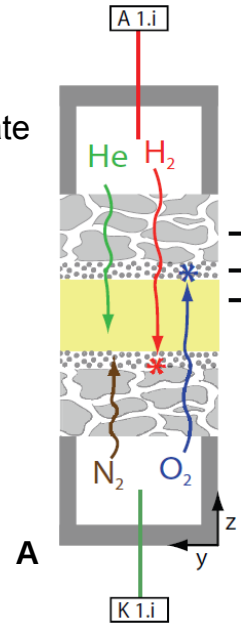

local permeation test wit He

G.A. Schuler, PhD thesis, ETH Zürich, 2010

Local Gas Phase Measurements Linear PEMFC

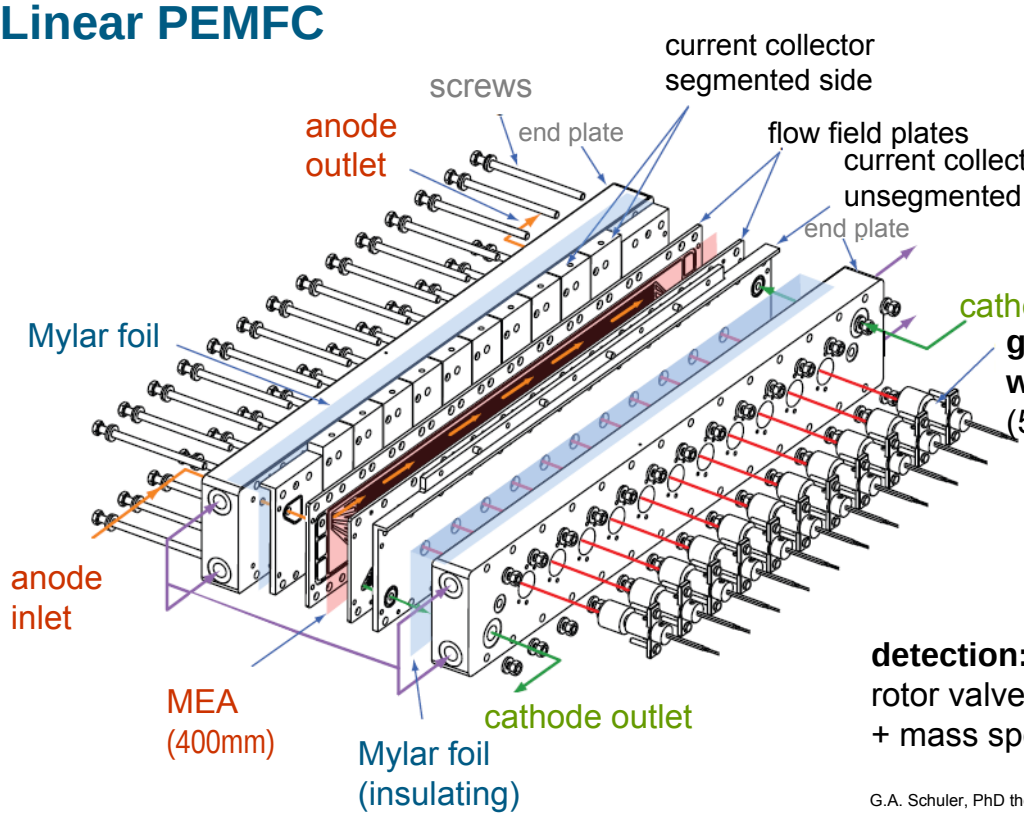

detection:
rotor valve
+ mass spectrometer

G.A. Schuler, PhD thesis, ETH Zürich, 2010

Local Gas Phase Measurements Linear PEMFC

local humidity measurement

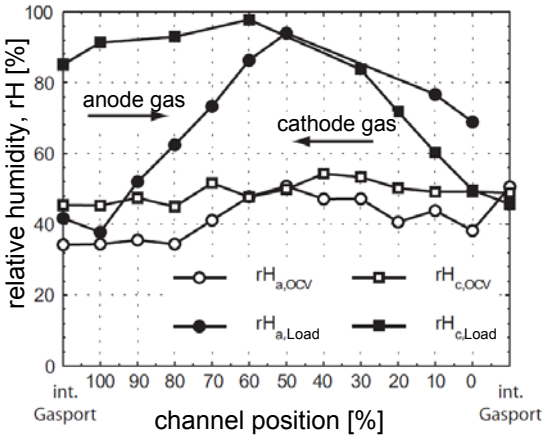

degradation during load cycles

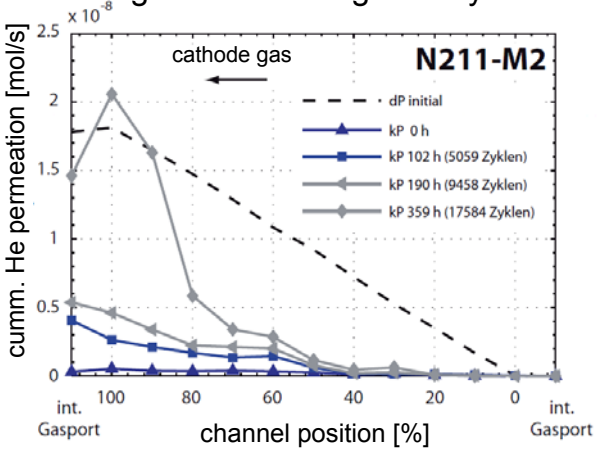

j=0 or 0.375 A/cm²; *T*=80°C;
anode: 90% H_2 / 10% He, rH=46%, λ=3
cathode: air, rH=50%, λ=2
p=1.5 bar_{abs};
condensation on cathode side (40-60%)

j=0 <->0.3 A/cm² (cycled: 30s, d*j*/d*t*=0.05A/cm²s); *T*=80°C;
anode: 90% H_2 / 10% He, rH=30%, λ=2
cathode: air, rH=30%, λ=2
p=1.5 bar_{abs};

G.A. Schuler, PhD thesis, ETH Zürich, 2010

4. Radiography & Tomography

Radiography

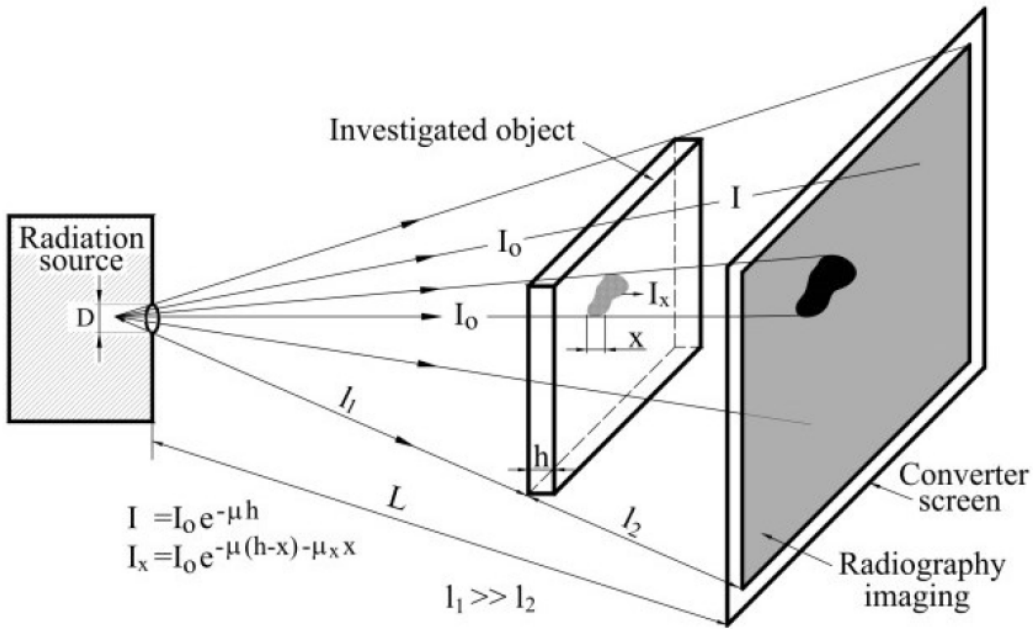

Unsharpness:

$$U_{\text{beam}} = \frac{l_2}{L/D}$$

$\Leftrightarrow$

Brightness (flux, s/n ratio):

$$\Phi_{\text{image plane}} = \frac{\Phi_{\text{source}}}{16 \cdot (L/D)^2}$$

Svab & Balasko: Physical Methods, Instruments and Measurements - Vol IV - Non-destructive Testing: Neutron Radiography

Element Specific Attenuation
X-Rays vs. Thermal Neutrons

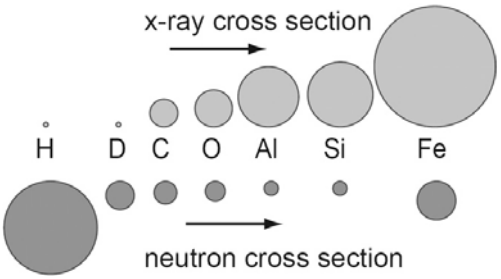

Satja et al., J. Power Sources 129 (2004), 238

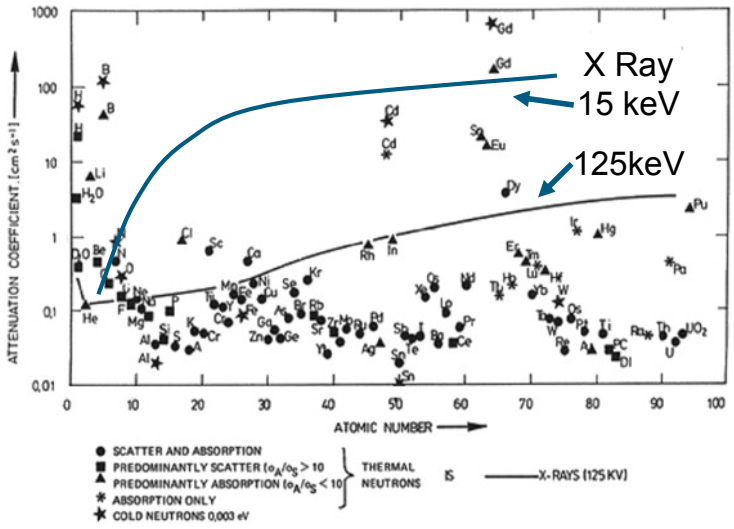

X-ray: ~ continuous increase with atomic number

neutrons:

- scattering attenuation for different elements (high att. for H,C,O)
- much larger penetration depth (100x) than synchrotron X-Ray (15 keV)

X-Ray Radiography
X-Ray Sources

X-Ray tube

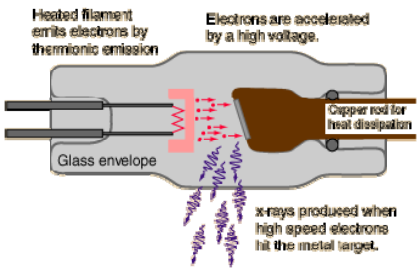

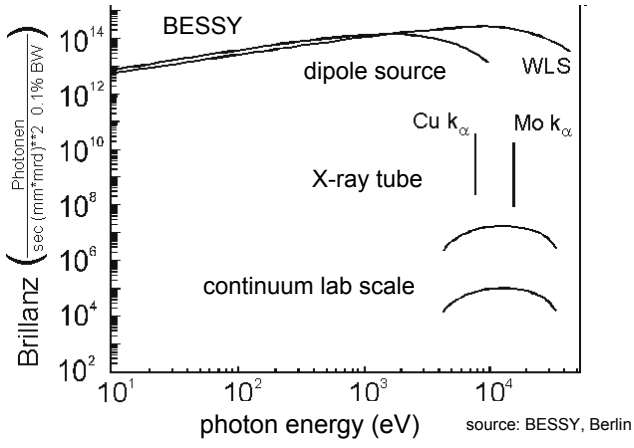

Synchrotron

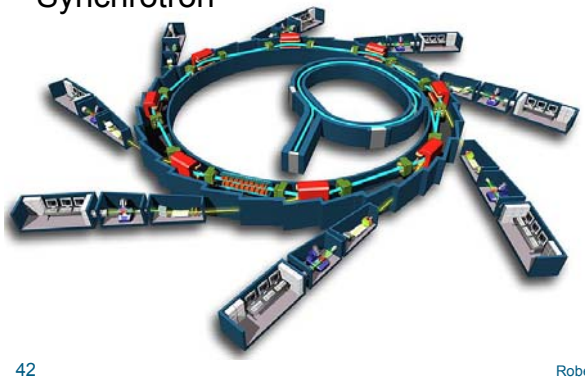

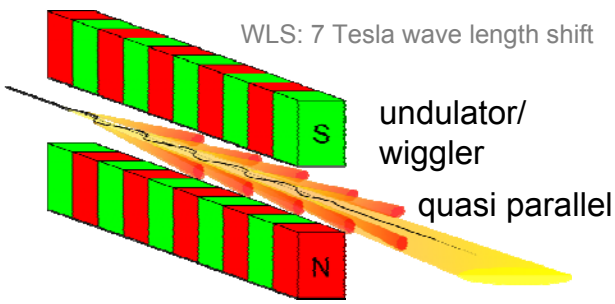

Computed Tomography

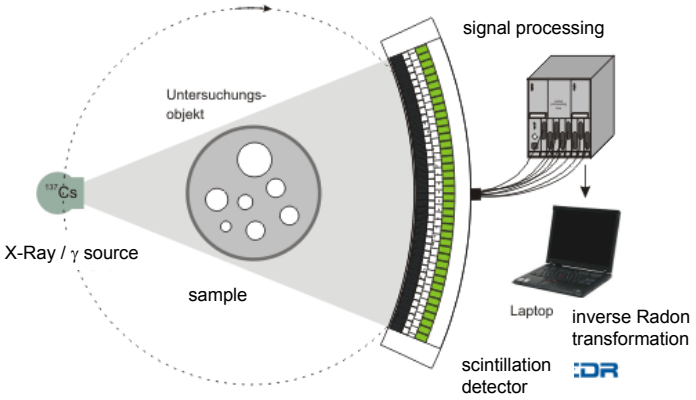

regular Radon transformation:

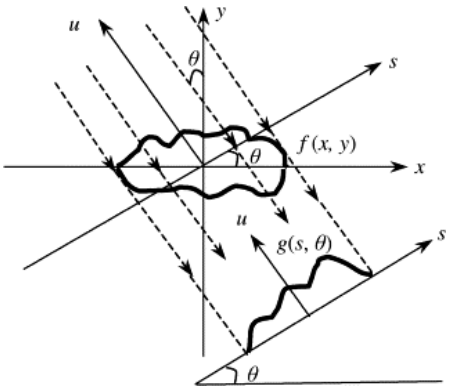

Y. Shao & M. Celenk, Pattern Recognition 34 [11] (2001), 2097-2113

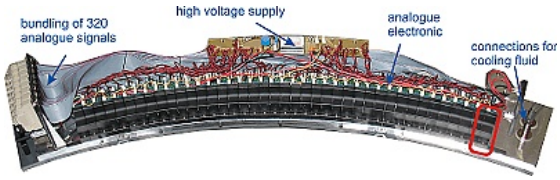

raw sinogram

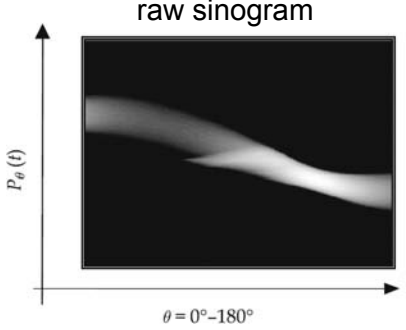

scintillator: reemit ionizing radiation as light
then detected by: photomultiplier, photodiodes, CCD …

Helmholz Zentrum Dresden

Computed Tomography

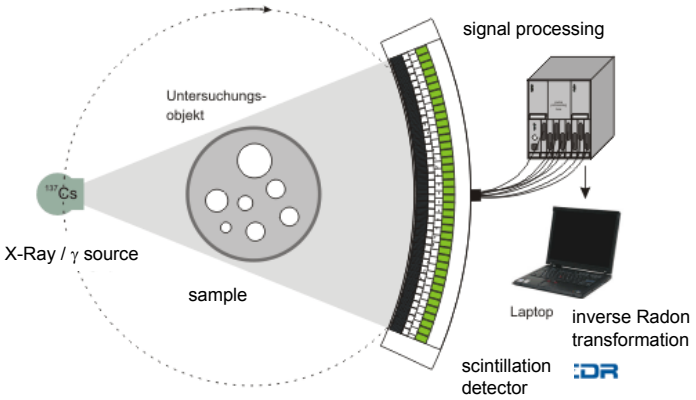

regular Radon transformation:

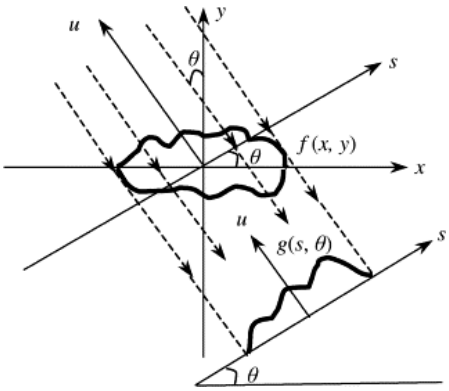

Y. Shao & M. Celenk, Pattern Recognition 34 [11] (2001), 2097-2113

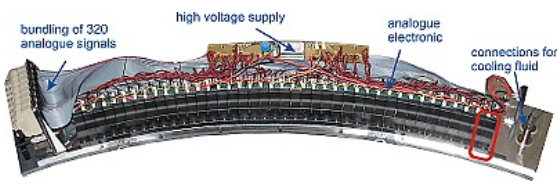

scintillator: reemit ionizing radiation as light
then detected by: photomultiplier, photodiodes, CCD …

Helmholz Zentrum Dresden

Reconstruction of a turbo clutch via filterted back projection

Tomography at Synchrotron

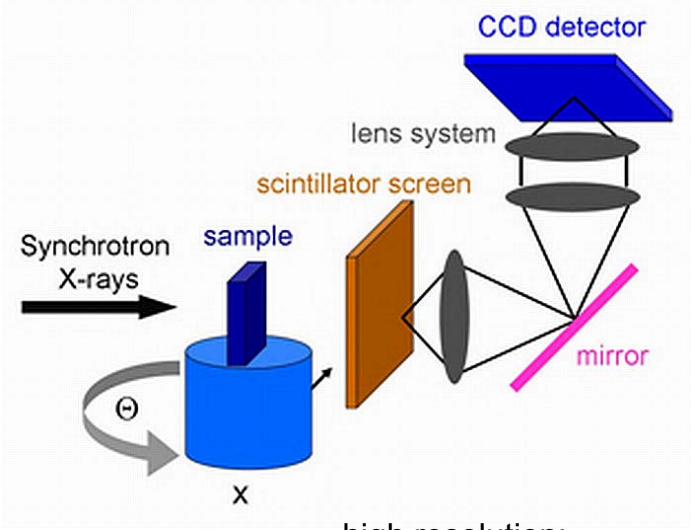

Helmholtz Zentrum Berlin

high resolution:
thin scintillators (50 µm)
required, e.g. $CdWO_4$
(applied on glass support)

CCD sensor
up to 12 MPx

e.g. 2 µm resolution
⇒ 8.5×5.5 mm² field of view

typical exposure time:
2-10s per angle projection

max. accuracy, if
number of angle projections
larger or equal
to CCD pixel width
(often lower due to scanning speed)

µ-CT vs. Synchrotron

Cone beam µ-CT 100 keV Synchrotron ESRF, ID15A

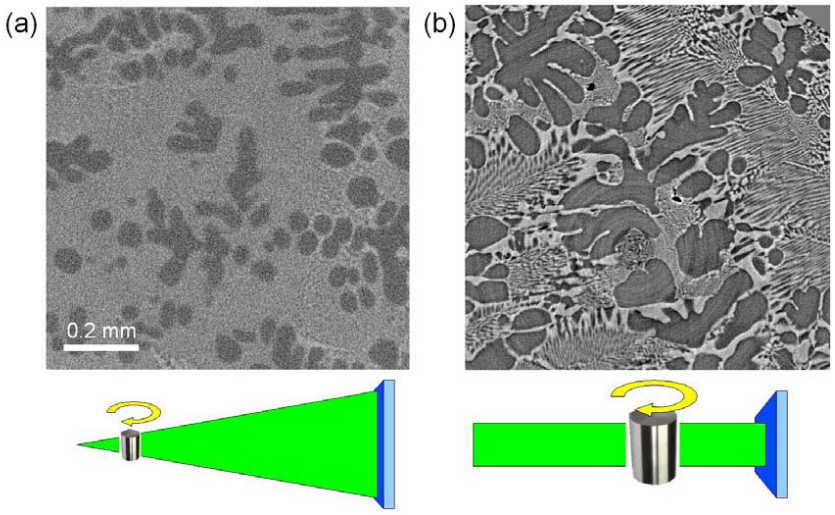

Al Cu alloy

voxel size	1.56 µm	0.7 µm
field of view	3.6 × 3.6 mm²	0.7 × 0.7 mm²
scan time	5.25 h	40 s
remark	beam hardening (low contrast, artefacts)	more details (eutectic system visible)

DLR Köln

Further Maximum Resolution Constrains (Stage)

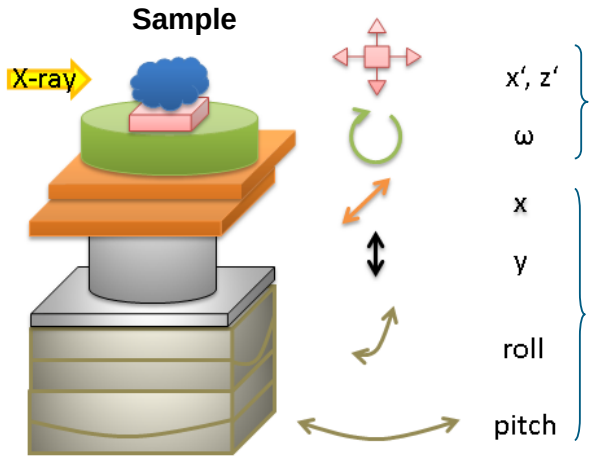

spot selection
tomographic rotation

alignment of rotation axis
relative to the beam
and detection system
(down-to 0.01°)

Stage setups at BAMline, BESSY, Berlin

	Micos UPR-160 AIR	Huber 410
eccentricity	0.1 µm	3 µm
max load	200 N	1450 N

T. Arlt, Ph.D. thesis, TU Berlin, 2012

X-Ray Tomography Example Water Detection in PEMFC

Cell & flow field adapted to fit beam dimensions (19.2×7.2)

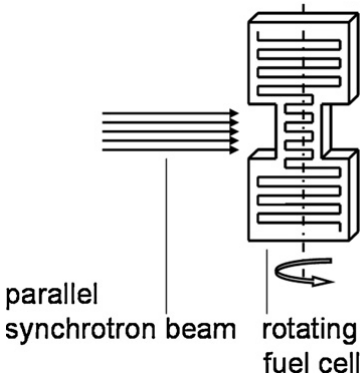

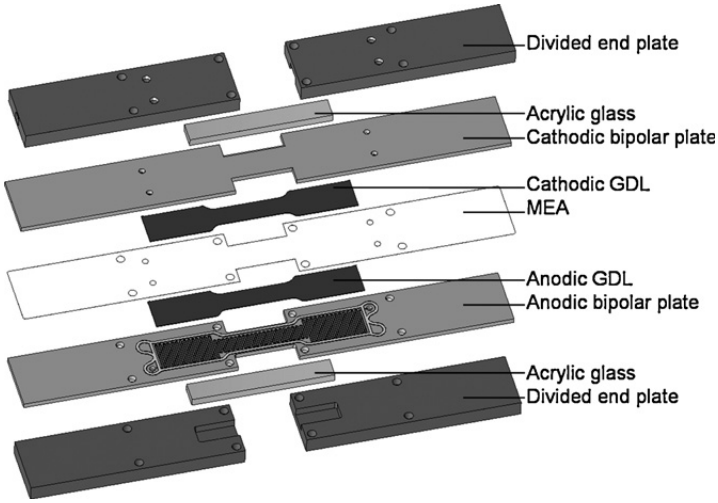

voxel size: 4.8 µm
1800 angle projections
60 min per tomogram,
closed inlets/outlet for tomography

No steel in analyzed area!
(would shield everything)
instead, use of acrylic glass in end plates
(other use e.g. graphite)

Krüger et al., J. Power Sources 196 (2011), 5250

X-Ray Tomography Example
Water Detection in PEMFC

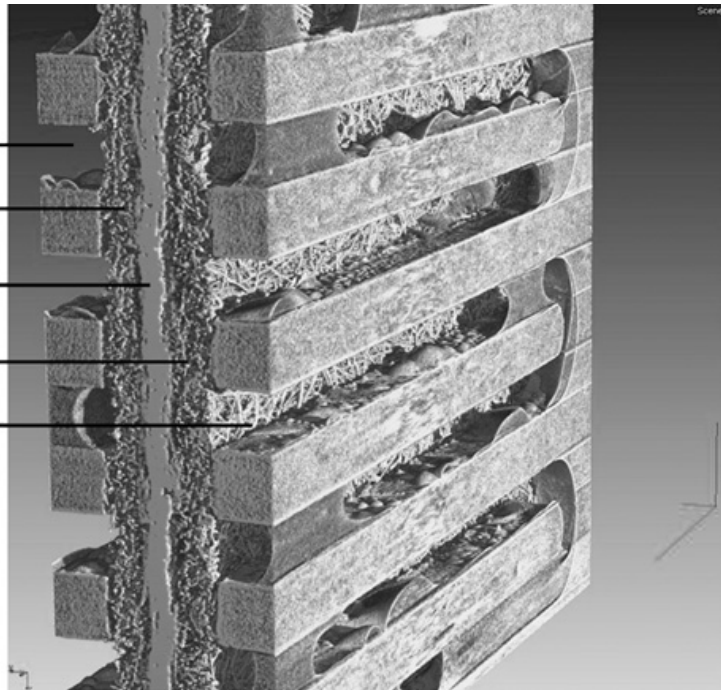

gravity caused
water droplets form
on bottom of ribs

anode: H_2, λ=2.0, humidified
cathode: air, λ=2.5, humidified
T=50°C, j=160 mA/cm²

Krüger et al., J. Power Sources 196 (2011), 5250

X-Ray Tomography Example
Water Detection in PEMFC

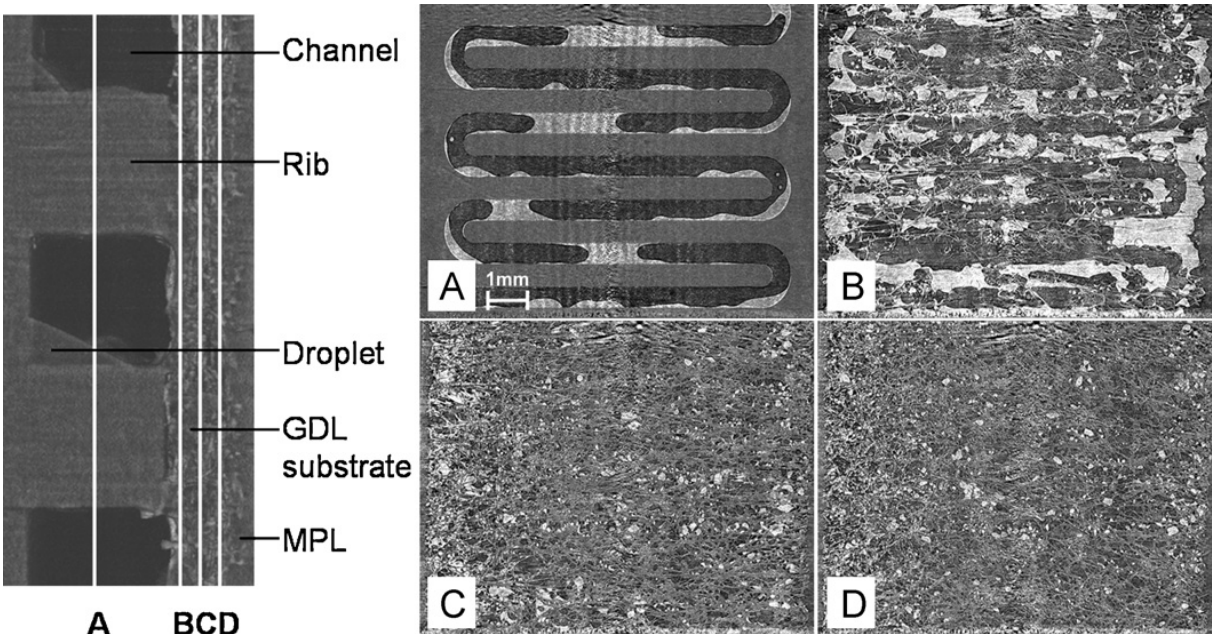

Krüger et al., J. Power Sources 196 (2011), 5250

X-Ray Radiography Example
Transient Water Detection in DMFC

Transient methods require **fast** acquisition
⇒ 2D radiography instead of 3D tomography
(exposure time ~0.4 s)

for reasonable signal/noise ratios and short exposure times: make everything **as thin as possible**

other way to get short exposure 2D radiogram / 3D tomogram:
use short times,
repeat experiment multiple times to get good signal/noise ratio
(requires triggering e.g. with current load)

thinning flow field plate
for in plane 2D radiography

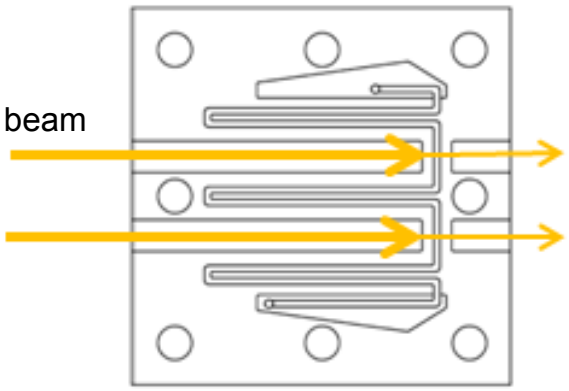

T. Arlt, Ph.D. thesis, TU Berlin, 2012

X-Ray Radiography Example
Transient Water Detection in DMFC

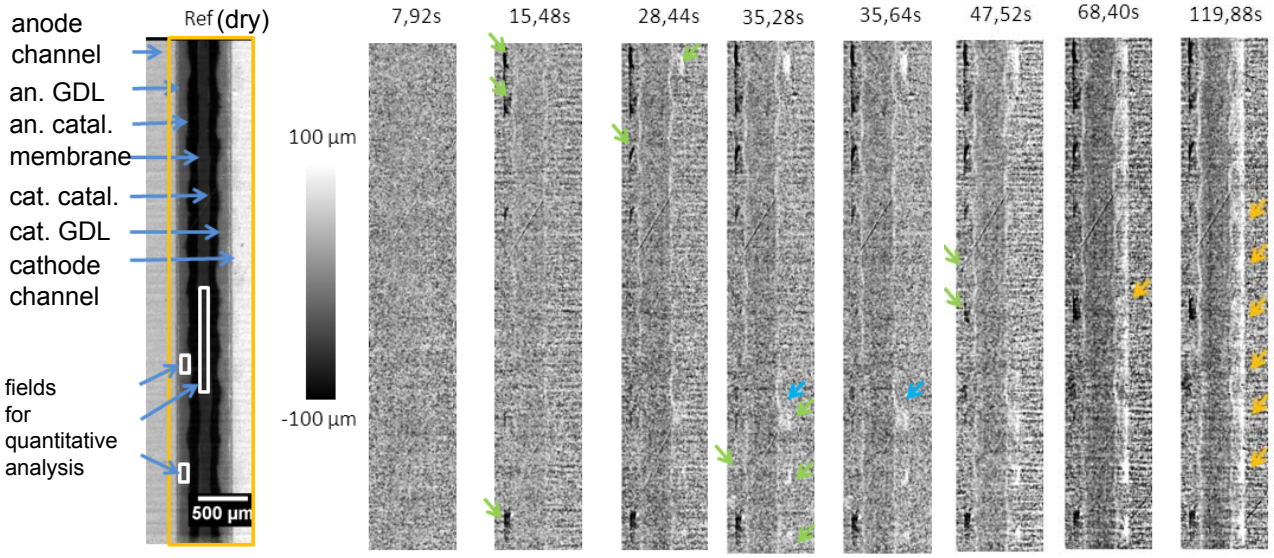

$\lambda_{an/ca}$t=4/4; *j*=150 mA/cm²; E=13 keV

anode: CO_2 bubbles
cathode: water droplets

decrease

periodic GDL fiber structure

T. Arlt, Ph.D. thesis, TU Berlin, 2012

X-Ray Tomography
Water Detection in HT-PEFC

no liquid water ⇒ traditional analysis fail

Indirect method:

Model from measured membrane transmission and thickness, and local phosphoric acid distribution

T. Arlt, Ph.D. thesis, TU Berlin, 2012

W. Maier et. al, Journal of The Electrochemical Society, 159 (8) F398-F404 (2012)

X-Ray Tomography Example (DMFC)
Ruthenium Corrosion / Combining with XAS

Transmission vs. Energy	21.7 keV	22.5 keV	differ-ence
Pt (3.2 µm)	0.660	0.686	3.9 %
Ru (0.8 µm)	0.989	0.938	-5.2 %
C (240 µm)	0.983	0.984	0.1 %
F (50 µm)	0.999	0.999	0.0 %

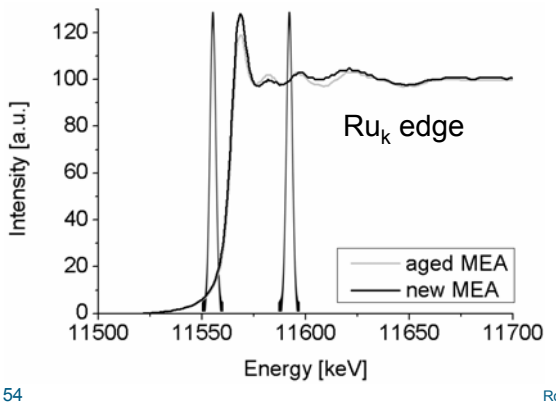

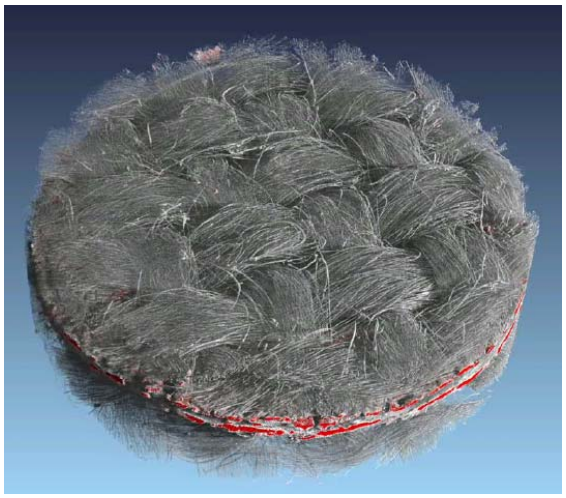

Ru in anode catalyst
overlay of quotient tomogram and absorption tomogram

i.e. measure two tomograms at different energies, divide them

T. Arlt, Ph.D. thesis, TU Berlin, 2012

X-Ray Tomography Example (DMFC)
Ruthenium Corrosion / Combining with XAS

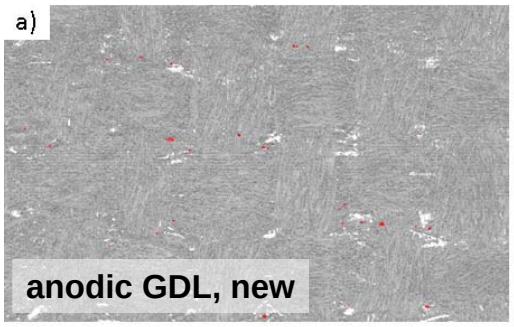

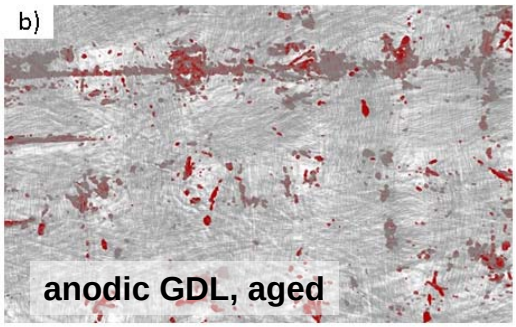

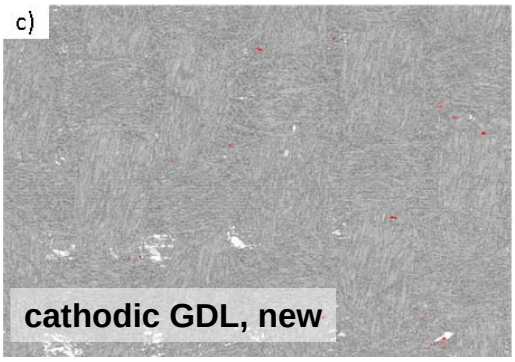

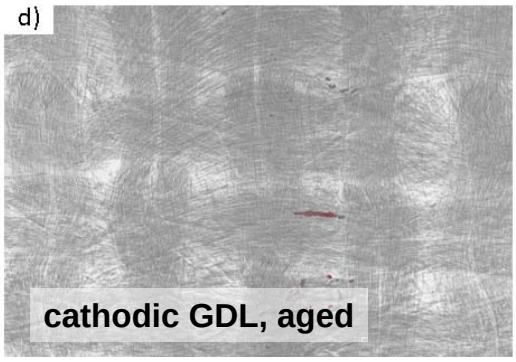

further finding:

more accumulation under lands/ribs

Neutron Radiography / Tomography

Fast neutrons:	10 keV - 20 MeV
Epithermal neutrons:	0.3 eV - 10 keV
Thermal neutrons:	**0.005 eV - 0.3 eV**
Cold neutrons:	<0.005 eV

Sources:
fission reactor or
spallation source (p accelerator)
with moderator

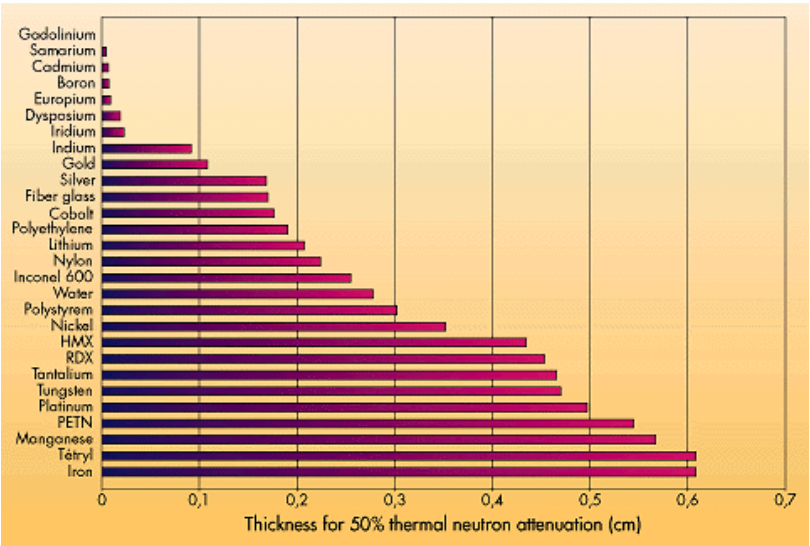

Penetration depth for different materials

•advantages over X-Ray
• different contrast
• no problem with Fe/steel
• typ. larger penetration
• no radiation damage

neutrons are difficult to focus
⇒ no completely parallel beam
⇒ limits resolution or flux

Neutron Radiography / Tomography Measurement Scheme

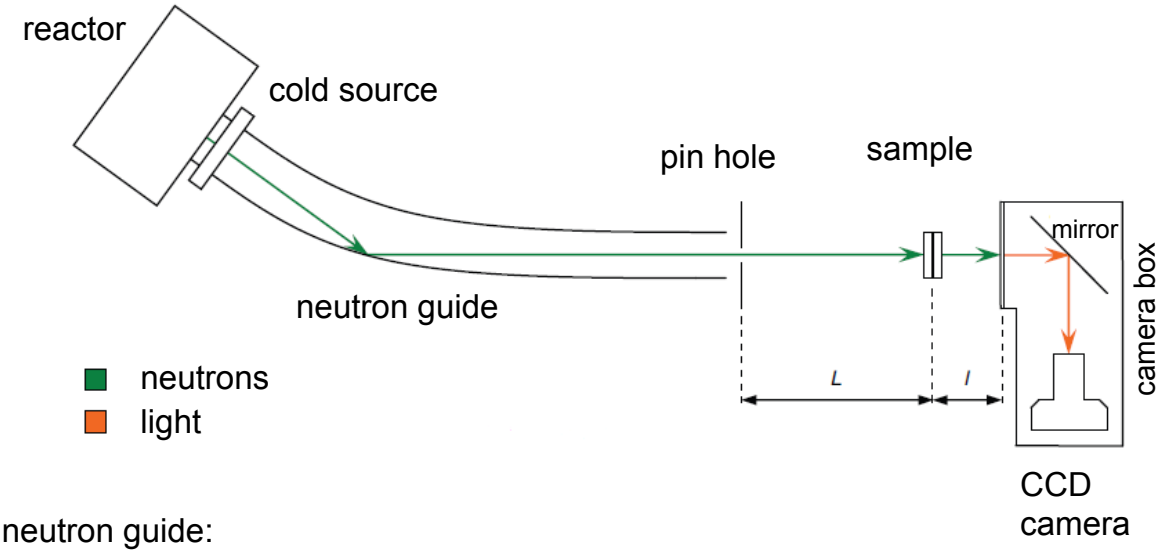

neutron guide:
- hollow glass tubes (total reflection)
- eliminates γ radiation background
- may possess elliptical end to focus

scintillators: $^{6}LiF+ZnS$ or Gd_2O_2S
Gd_2O_2S: 10 µm absorb 90% of flux
lower free paths of conversion electrons (higher spatial resolution)

A. Schröder Ph.D. thesis, FZ Jülich, RWTH Aachen, 2012

Neutron Tomography

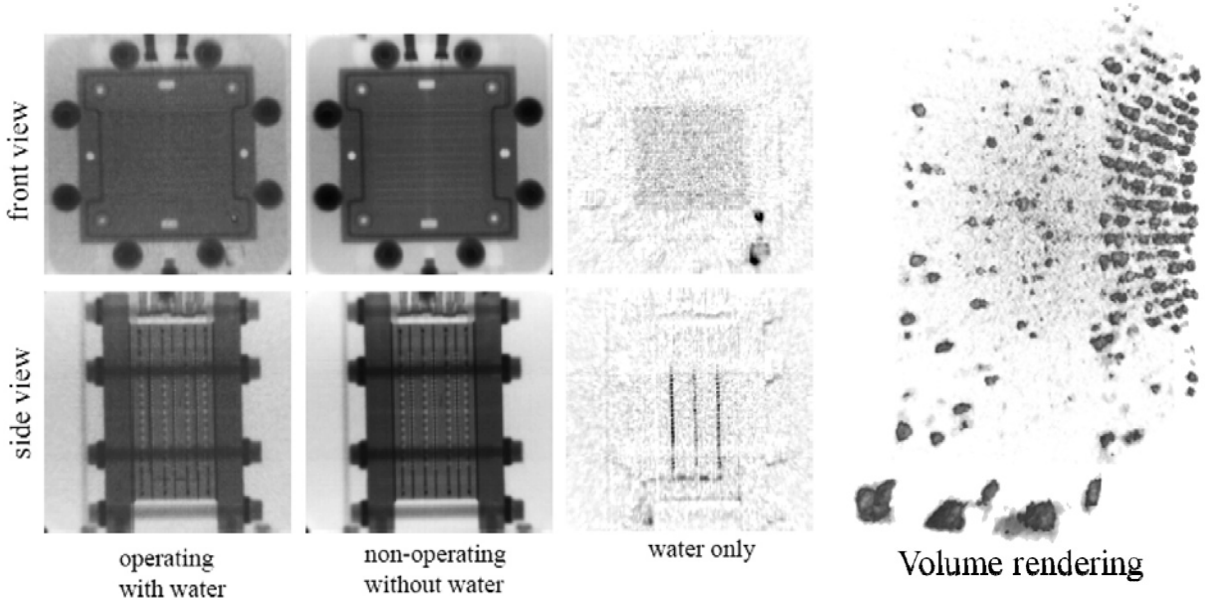

3 cell stack (52x52mm²)

applications:
process visualization, water quantification, flow field plate optimization

Takenaka et al. Nuclear Instruments and Methods in Physics Research A651(2011)277–281

Nuclear Magnetic Resonance Tomography (NMR)

Nuclear Magnetic Resonance Tomography

medium - high magnetic field devices requires (2-14T)
typical pixel numbers: 128x128 (rather low)
resolution: 1-6 µm
no ferro-magnetic materials

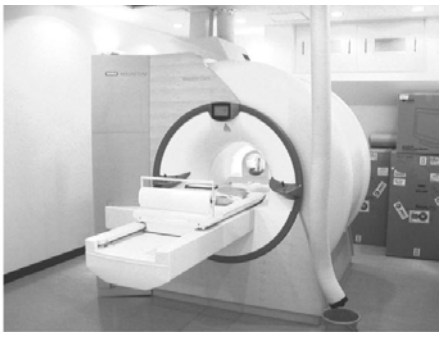

5. X-Ray Diffraction and Spectroscopy

X-Ray Diffraction Analysis

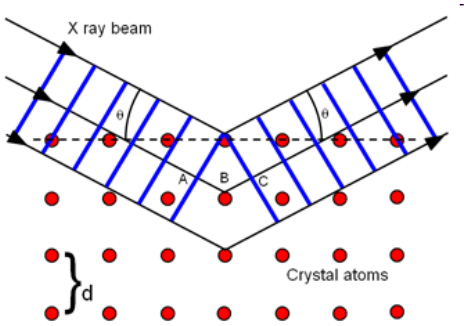

constructive interference
(Bragg equation):

$$n \cdot \lambda = d \cdot \sin\theta$$

results:
XRD diffractogram (is not a spectrum,
fixed wavelength, Cu-Kα radiation, 0.15nm)
chemical phases
(crystallographic system, with database)
unit cell parameters
⇒ strains ⇒ stresses (e.g. $\sin^2\psi$ method)

limits:
only crystalline phases
(no amorphous, no organics)

X-Ray Diffraction Analysis
In situ Analysis of SOFC Reduction Cycling

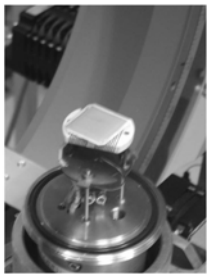

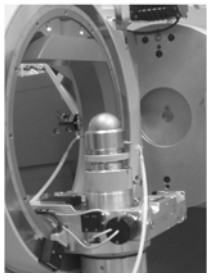

diffractogram

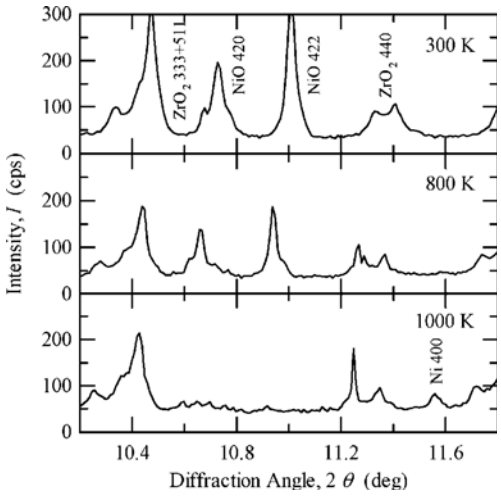

stress results

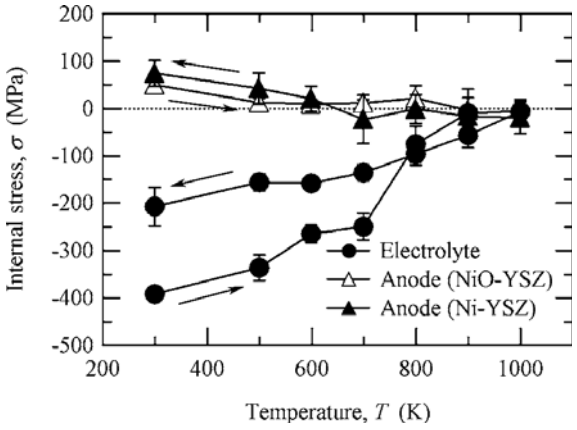

manufactured NiO
reduces above 800K

Sumi et al., Trans. ASME 3 (2006), 68

X-Ray Spectroscopy
XAS, EXAFS, XANES, XPS

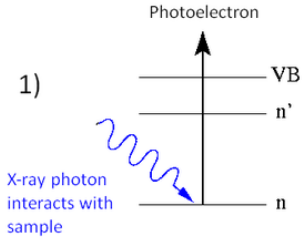

X-Ray photon spectroscopy (XPS):
= electron spectroscopy for chemical analysis (ESCA)

kinetic energy of photoelectrons (only top 20 at. layers)
considering ionization energy ⇒ (app.) binding energy

X-Ray Absorption Spectrum (XAS)

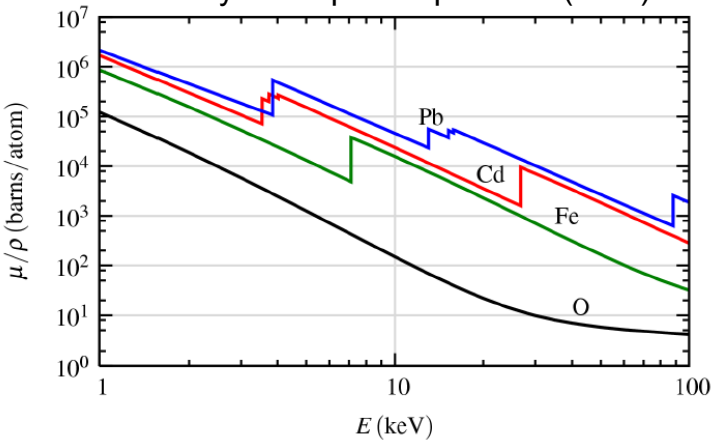

detection by e.g. single crystal monochromator
with photomultiplier
(counts per wavelength)
high resolution (<5 eV)
similar to Wavelength Dispersed X-Ray Analysis (WDX)

Energy dispersed X-RAY analysis (EDX) of X-Ray photons after fluorescence
Si based detectors (U form E_v)
low resolution (150..600 eV):

X-Ray Spectroscopy
XAS, EXAFS, XANES

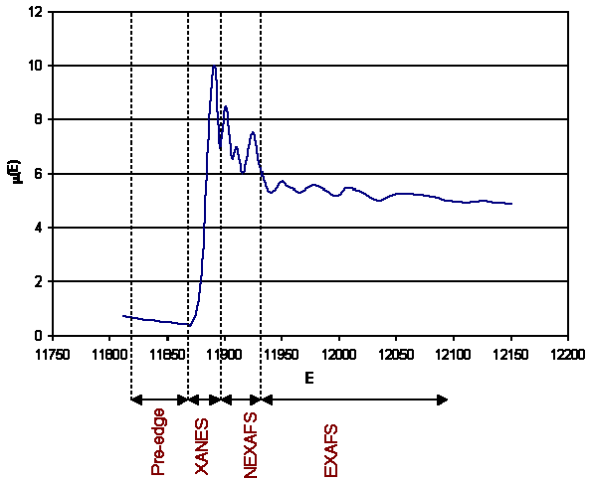

X-Ray Absorption Spectrum (XAS)

- X-Ray Absorption Near Edge Spectrum (XANES)
- Near Edge X-RAY Absorption Fine Structure (NEXAFS)
- Edge X-RAY Absorption Fine Structure (EXAFS)

influenced by oxidation level, neighborhood (spin coupling)

oxidation level shift edge in XANES region

used to determine oxidation level of Fe in $La_xSr_{1-x}Co_yFe_{1-y}O_{3-\delta}$ (~2.5 ⇒ δ=~0.5)

no provable oxidation of Mn in LSM

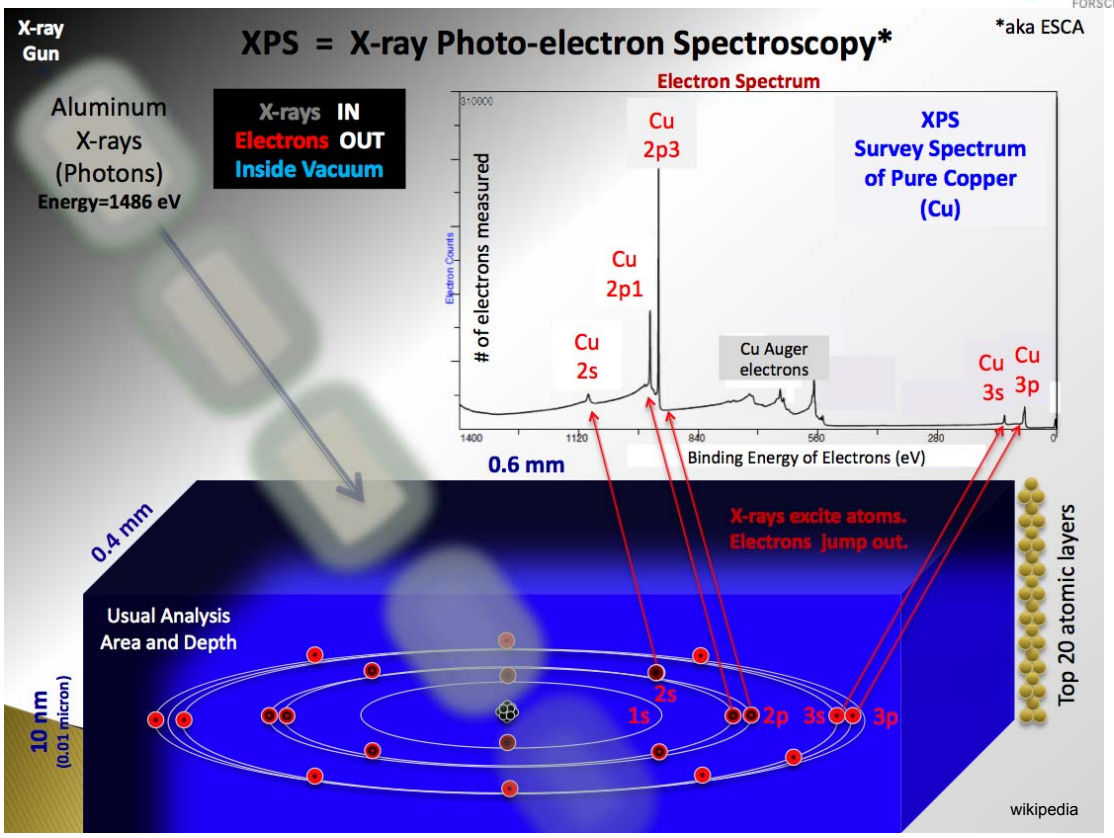

Ce Oxidation State with XPS

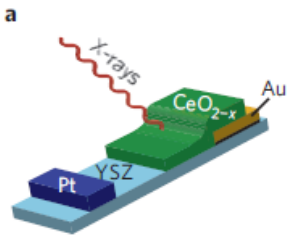

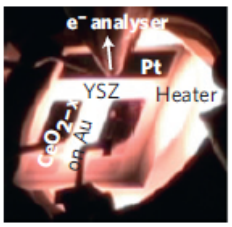

single chamber fuel cell/electrolyser

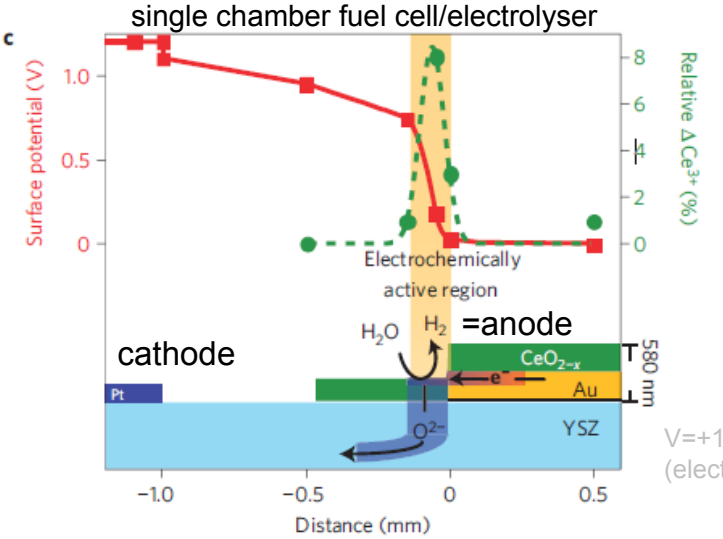

CeO_2: normally Ce^{4+}

but may be reduced to Ce^{3+}:

$$2Ce^{4+} + O^{2-} + H_2(g) \Leftrightarrow 2Ce^{3+} + V_O + H_2O$$

CeO_{2-x}: mixture Ce^{4+} & Ce^{3+}

contact less potential measurement by change in kinetic energy due to local potential V_L

$$\Delta E_{kin} = e \cdot V_L$$

Zhang et al. Nature Materials 9 (2010), 944

Ce Oxidation State with XPS

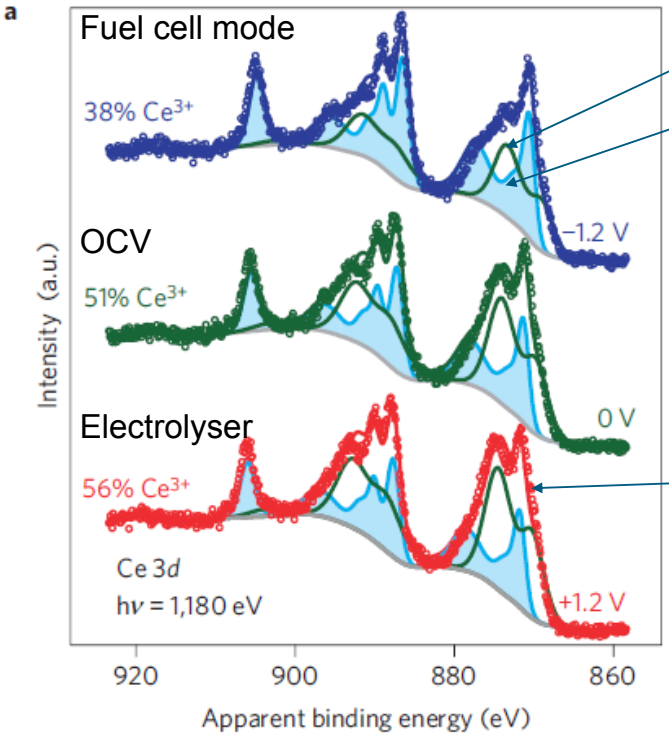

Ce^{4+}

Ce^{3+}

most Ce^{3+} for most reducing conditions

observed superposition

Zhang et al. Nature Materials 9 (2010), 944

Ce Oxidation State with XPS

shift due to local potential

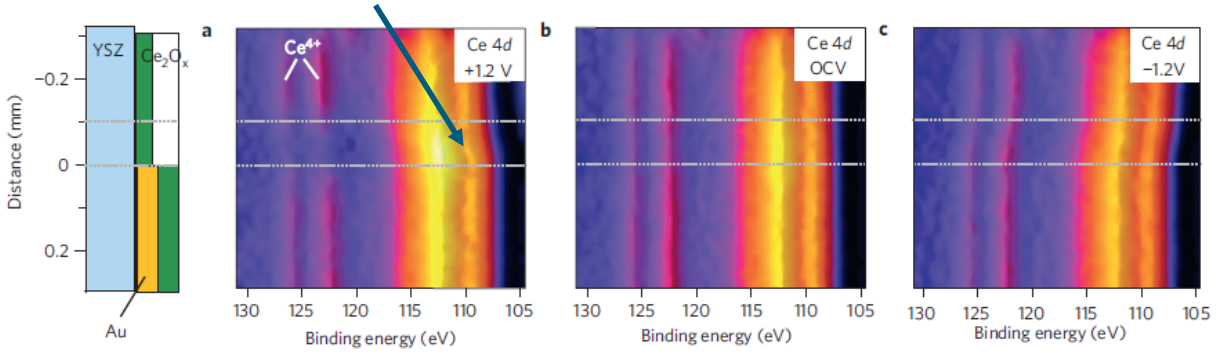

electrolyser mode
Ce^{4+} disappear in active region

OCV
homogeneous

fuel cell mode
homogeneous

Zhang et al. Nature Materials 9 (2010), 944

6. Raman Spectroscopy

Raman Spectroscopy Principle

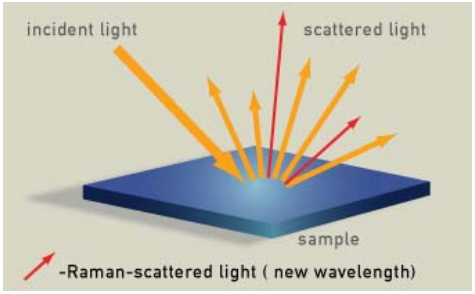

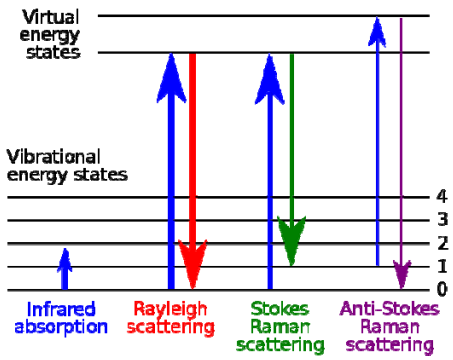

elastic scattering types

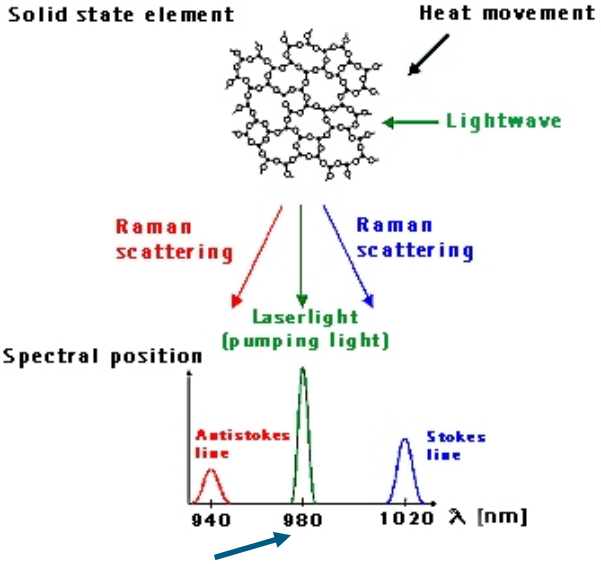

fixed excitation wave length (typical: NIR)

shifts=f(molec. rotations, vibrations, electronic transitions, temperature, stress)

=finger print of material and chemical composition

In situ Setup for SOFCs

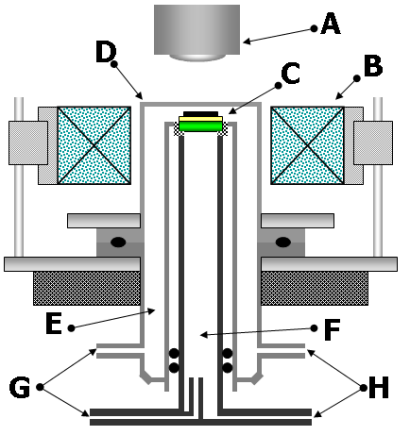

A: Objective lens
B: Heater
C: Anode supported type cell
D: SiO_2 glass chamber
E: Air side
F: Fuel side
G: Gas in
H: Gas out

most difficult part:
optical access without changing
(too much of) the operating conditions

can be extended for
3D structures (roughness)
by **confocal imaging**

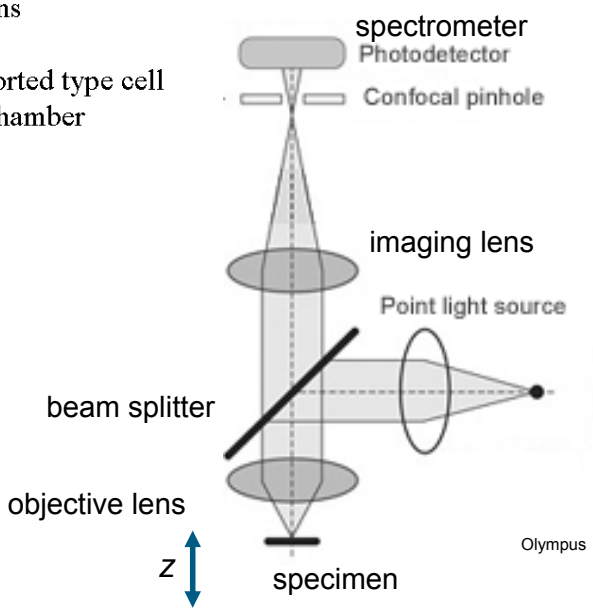

Nagai et al.,ECS Transactions, 35 (1) 519-525 (2011)

Temperature Dependence of Raman Shifts

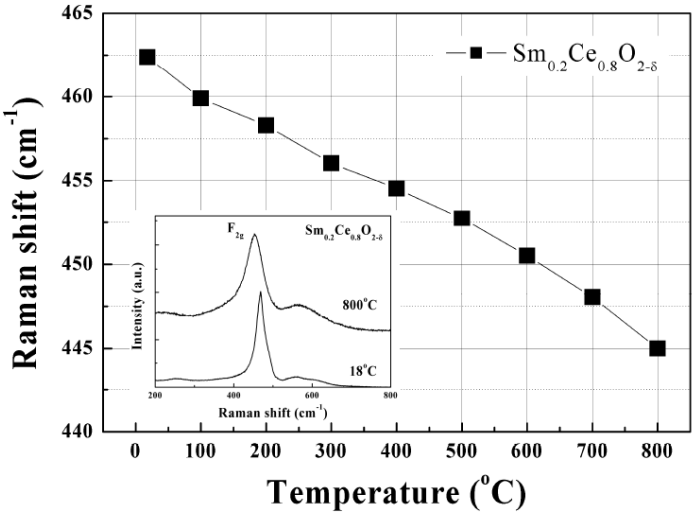

Grüneisen parameter
(lattice volume V, photon frequ. ω)

$$\gamma = -\frac{\partial(\log \omega)}{\partial(\log V)}$$

thermal expansion changes
lattice

Nagai et al.,ECS Transactions, 35 (1) 519-525 (2011)

Raman Shift
Stress Calculation

volume change due to in plane stress σ

$$\frac{dV}{V} = \left(1 - \frac{2\nu}{E}\sigma\right)\left(1 + \frac{1-\nu}{E}\sigma\right)^2 - 1$$

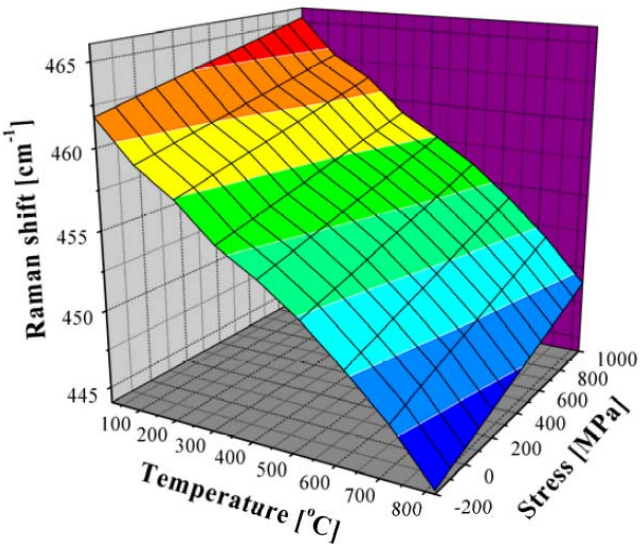

much more sensitive to temperature than to stresses =>
accurate temperature measurement necessary

Nagai et al.,ECS Transactions, 35 (1) 519-525 (2011)

Raman Shift
Stress Measurement Example

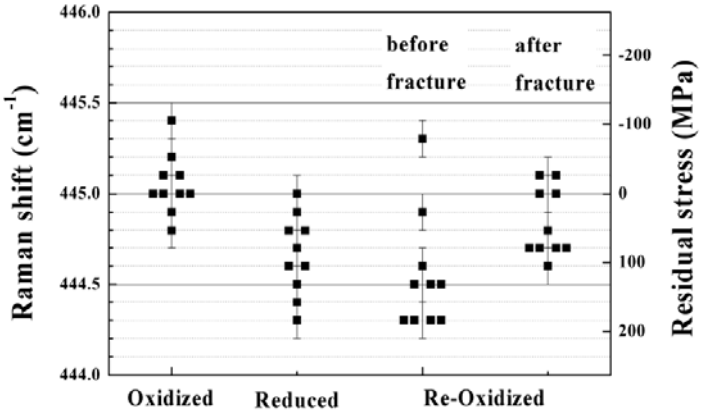

better would be in situ XRD
(smaller error:
approx. 20-50 MPa)

Nagai et al.,ECS Transactions, 35 (1) 519-525 (2011)

Carbon Detection
SOFC Fuel Oxidation

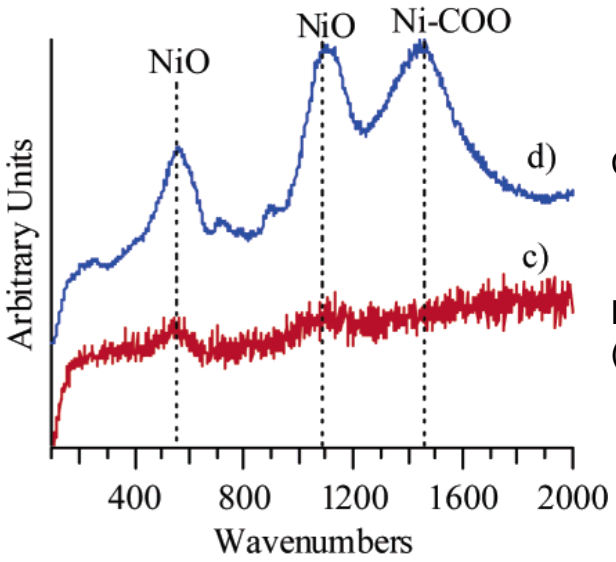

CO fuel

H2 fuel
(4x exaggerated)

Intermediate
Ni-COO
formation

further used for
detection of
- graphite
- NiS
- swelling of Nafion

Pomfret et al., Anal. Chem. 79 (2007), 2367-2372

μ Raman:
lateral resolution: 0.5-1 μm
information depth: 1.5 μm

7. Scanning Probe Microscopy

Scanning Probe Microscopy (SPM)

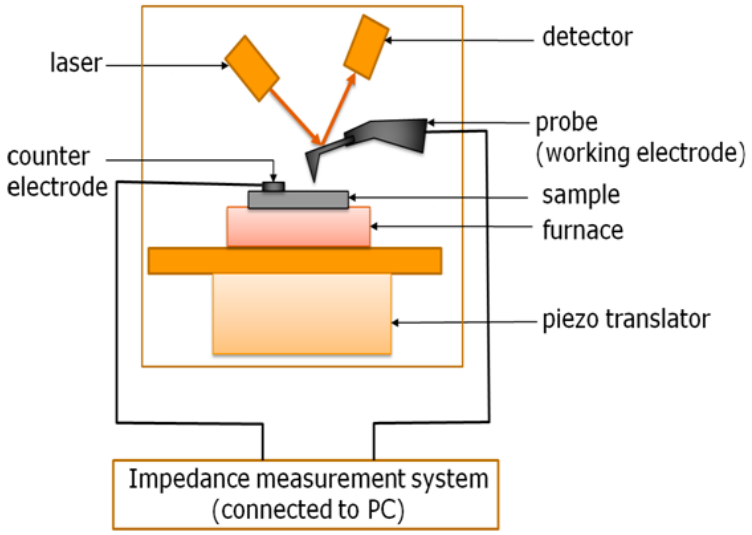

Simultaneous recording of topography as well as conductivity images

Topographical images are obtained like in a normal AFM in contact mode

In situ electrochemical impedance spectroscopy (EIS) measurement can be done using the probe as a working electrode

Controlled Atmosphere High Temperature SPM

Balasingam, Risoe

Scanning Probe Microscopy (SPM)

YSZ with LSM/YSZ probe

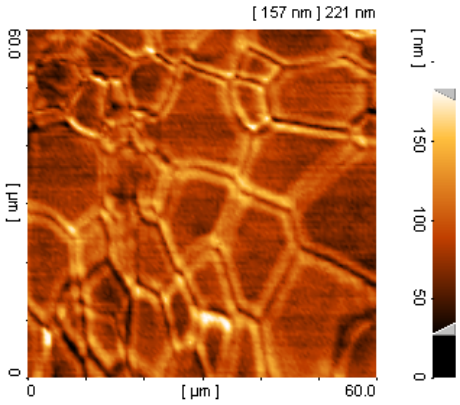

Micro impedance

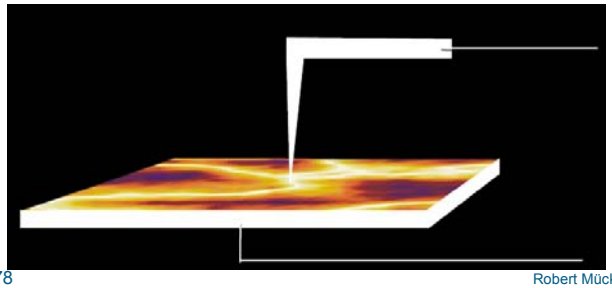

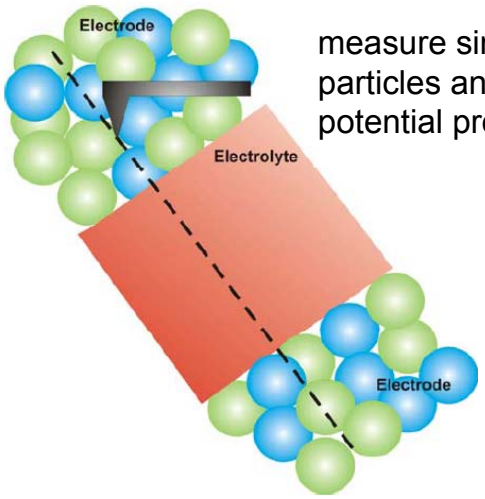

measure single particles and potential profiles

Current development stage:

probe/tips, micro electrodes, µ-EIS

Summary

- Virtually all *ex situ* methods can be applied *in situ* with certain restrictions, thereby large improvement of understanding
- However, most *in situ* methods require special setups (cells, stacks components, no out-of-the-box stacks etc.)
- Modification should be evaluated (same behavior as normal)
- Only electrochemical methods allow in-situ characterization of any system without modification
- Many methods allow similar investigations with different resolution and experimental afford
- Many in situ methods are expensive, can therefore not be used for everyday business/benchmarking, only for well planed purpose
- Theoretical background (what do I see?) can be quiet comprehensive (speak with experts)